Bayesian Brain Tissue Segmentation using a Subject Specific Atlas Priors

Colin Studholme
Biomedical Image Computing Group
http://depts.washington.edu/bicg

Depts. Pediatrics, Bioengineering, Radiology,
University of Washington

Overview

- Automated MRI Brain Tissue segmentation:
  - Motivation
- MRI tissue segmentation algorithms:
  - Gaussian Mixture models for MRI tissues
  - EM Based Tissue labeling
  - Spatial Priors
- Subject Specific Priors
  - Parameterization of Anatomical Priors
  - Modeling of probabilities
  - Example in Brain development
- Applications of Automated Segmentation:
  Human Fetal Brain Morphometry

Motivation

- Brain MRI scans reveal basic tissue structures:
  - Grey Matter, White Matter, CSF
- Need to extract tissues to quantify brain anatomy:
  - Total, Regional and Local Volume
  - Surface Curvature
  - Cortical thickness
- Detect brain tissue changes:
  - atrophy, tissue loss
    - (eg provide biomarkers for drug treatments of Alzheimer's disease)
  - Growth and abnormal development

Brain tissues and MRI intensities

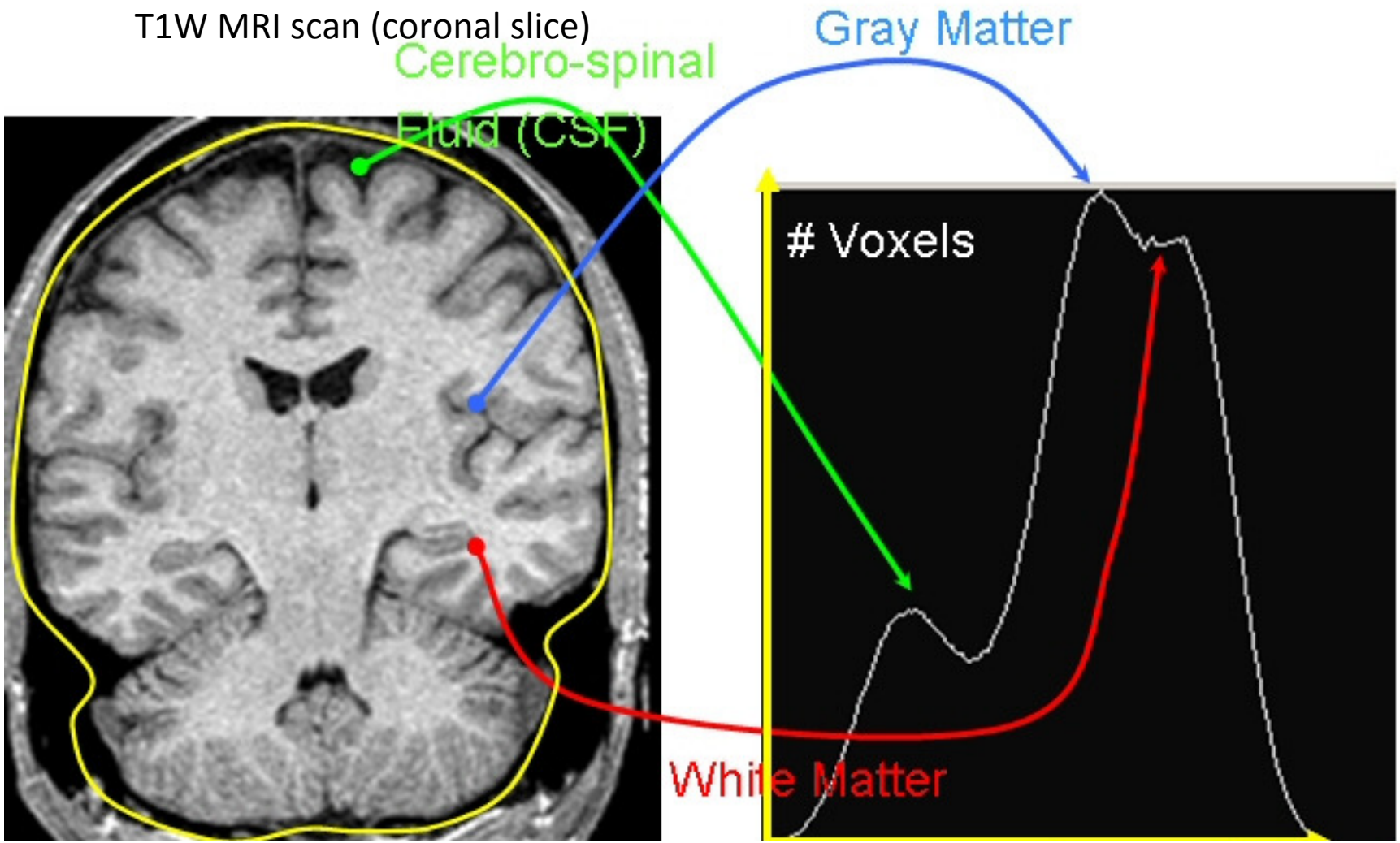

Tissue Classification

Key assumption:
Tissue classes appear as piece wise uniform regions of intensity

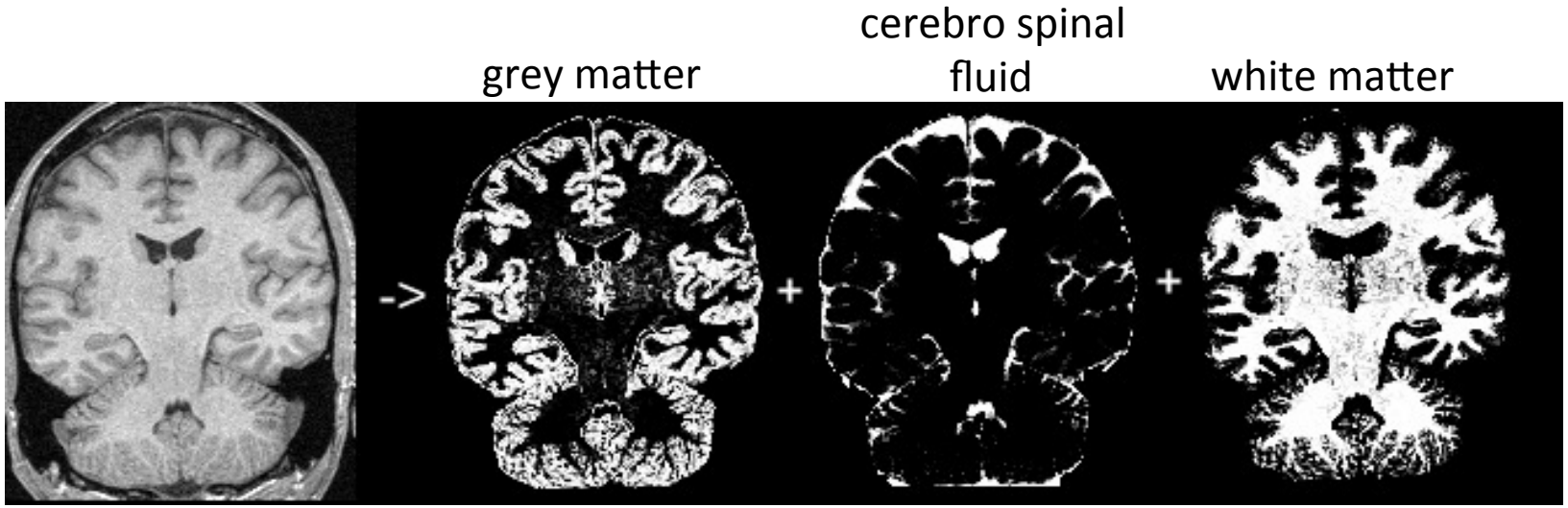

The Image Intensity: Observed data (voxel values)

Observed Tissue Intensity in the given MRI

voxel $j=1$ ...

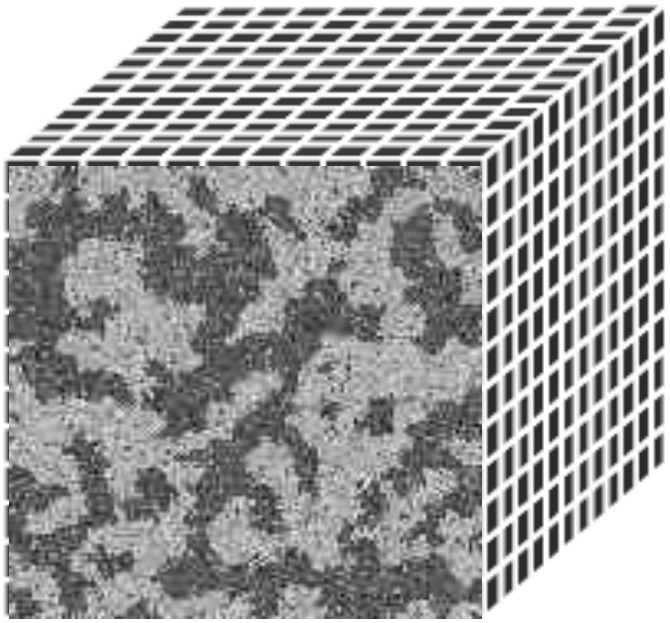

... voxel $j=n$

The set of voxel values together:

$$Y = \{y_1, \ldots, y_n\}$$

is a realization of an n dimensional Random Variable

$$Y = (Y_1, \ldots, Y_n)$$

Each individual voxel intensity y_i can be treated as a realization of a random variable $\mathrm{Y_j}$ where y_j is from the set of tissue intensities appearing in the image (eg 0-255 or 0-65535)

The Tissue Labels: 'Hidden' data

Tissue Types in the Underlying Anatomy

voxel $j=1$ ...

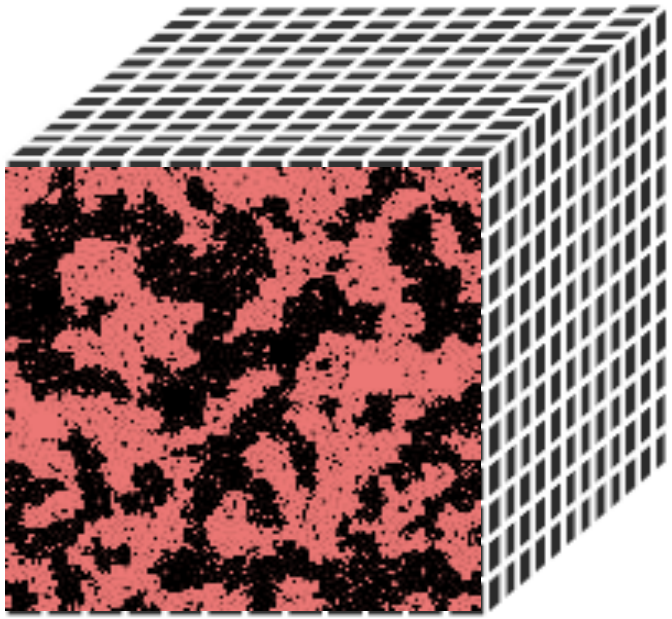

... voxel $j=n$

(Here two tissue classes: red and black)

The set of voxel labels together:

$$L = \{l_1, \ldots, l_n\}$$

is a realization of an n dimensional Random Variable

$$L = (L_1, \ldots, L_n)$$

Each individual voxel label l_i can be treated as a realization of a random variable $\mathrm{L_j}$ where l_j is from the set of tissue classes appearing in the image (e.g. grey matter, white matter etc)

For a Voxel: The conditional probability density of intensity y_i occurring, given tissue label is k

For most classes it is reasonable to assume a Gaussian/Normal distribution:

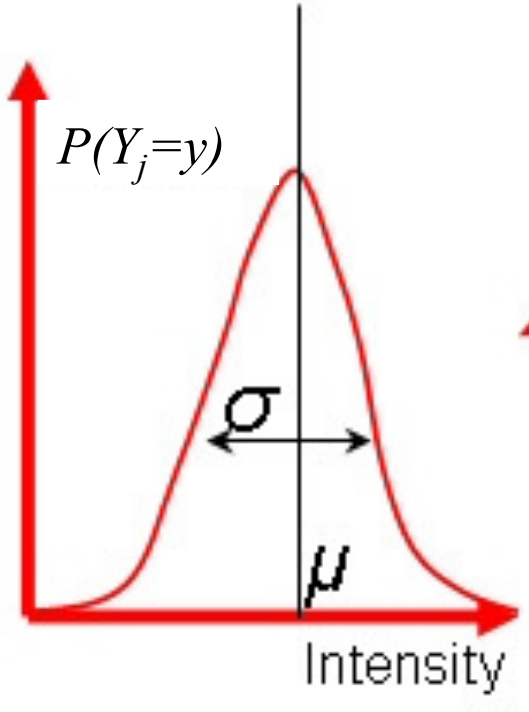

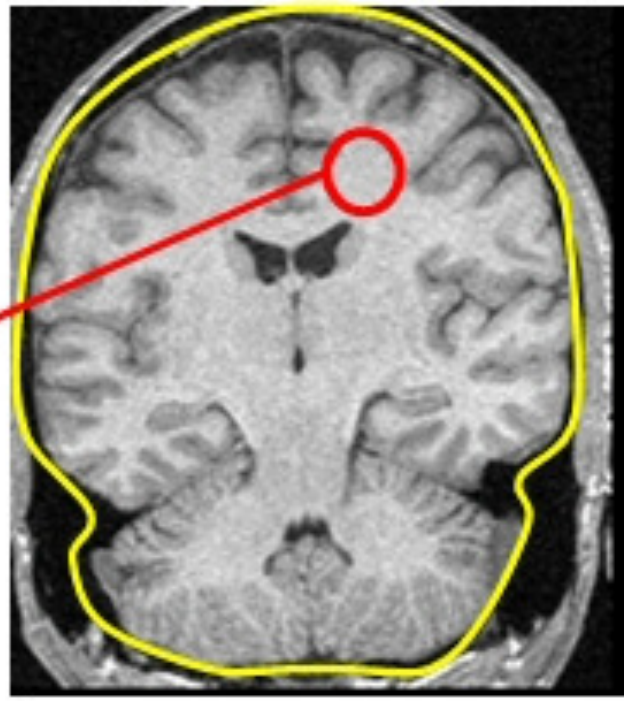

$$p(Y_j = y \,|\, L_j = k, \Phi) = G(y, \mu_k, \sigma_k) = \frac{1}{\sqrt{2\pi}\sigma_k} e^{\frac{(y-\mu_k)^2}{2\sigma_k^2}}$$

$$\Phi = \{\mu_k, \sigma_k\}$$

Parameters determining the distribution: in general we don't know these: MRI scans do not provide calibrated intensities (unlike CT)

The Probability density of random variable Y_j

Given by the sum of probabilities of each tissue class
(a Gaussian Mixture Model)

$$p(Y_j|\Phi) = \sum_{\forall k} p(Y_j|L_j = k, \Phi)\, p(L_j = k|\Phi)$$

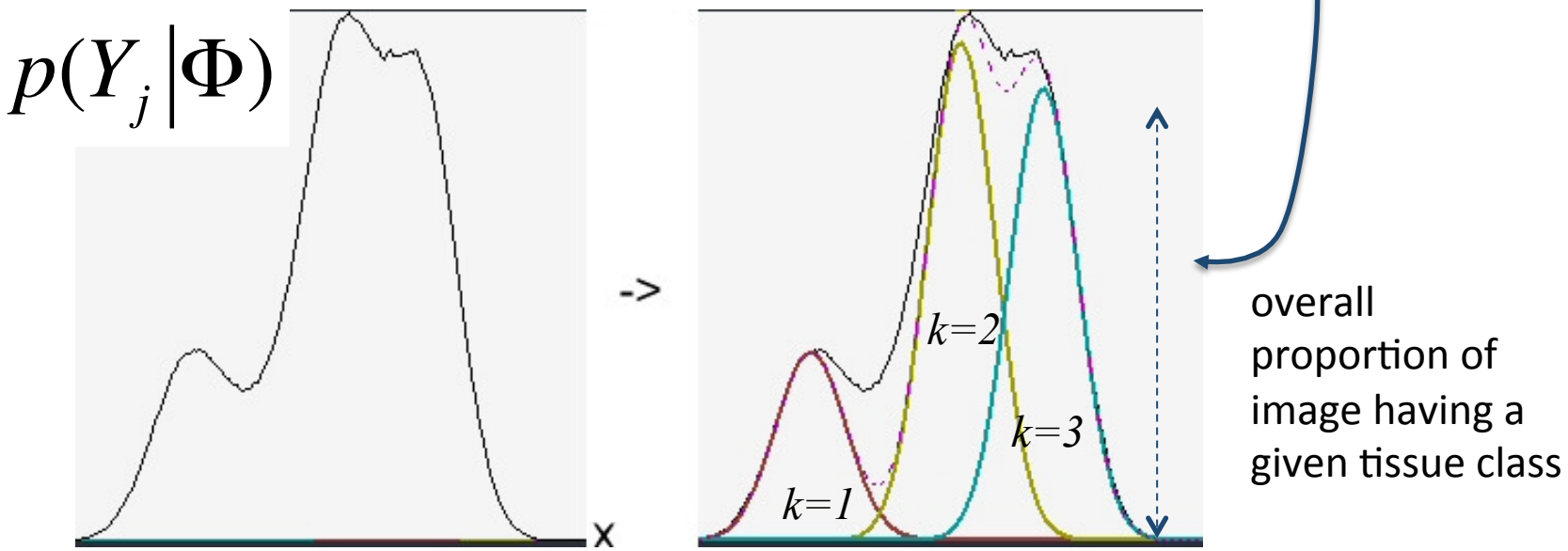

Probability density of random variable Y_i

Assuming that the prior probability of voxel at j belonging to tissue class k is spatially constant:

$$p(L_j = k \mid \Phi) = c_k$$

This acts as a 'Mixture Weight' for each class k in the Gaussian Mixture Model:

$$p(Y_j \mid \Phi) = \sum_{\forall k=1..K} p(Y_j \mid L_j = k, \Phi) c_k$$

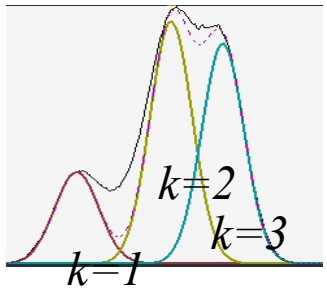

The total set of parameters to be estimated for all possible tissues is then:

$$\Phi_{ALL} = \{\mu_1, \sigma_1, c_1 ..... \mu_K, \sigma_K, c_K\}$$

Together with the tissue Labels for the voxels:

$$L = \{l_1, ..., l_n\}$$

->How to find values for these?

Probability of observing a whole MR image given underlying tissue labels

Assume that the intensity of a voxel given its tissue label, is
conditionally independent from the intensity of other voxels
(i.e. the random variables $Y_1, Y_2 \ldots Y_n$ are independent)

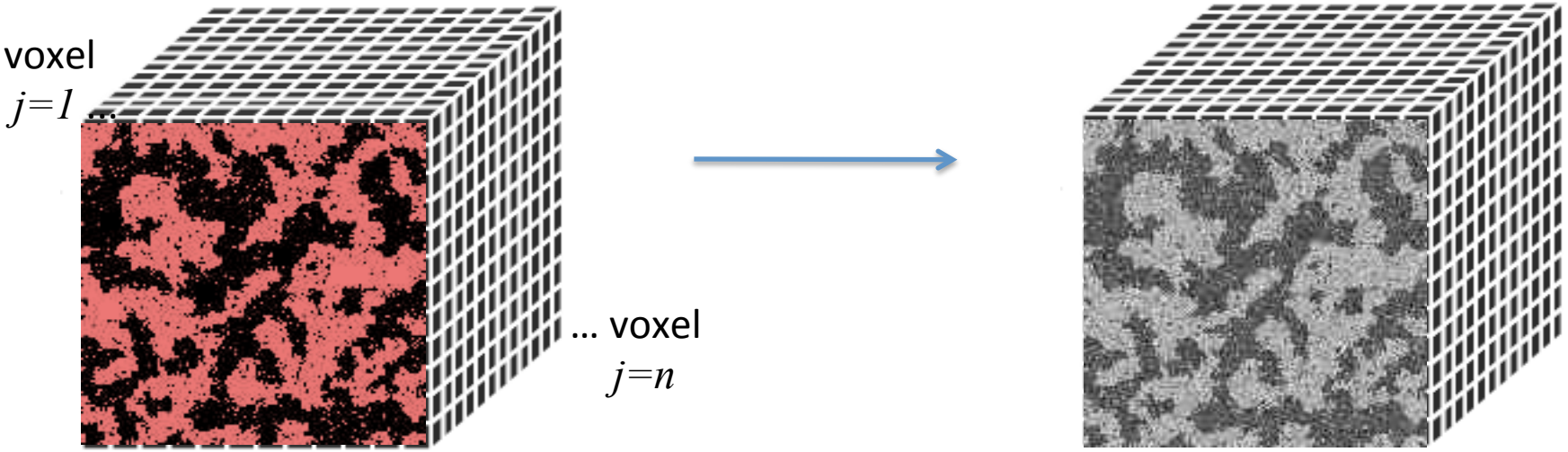

Then:

The probability of observing an image Y given a set of labels is the product of observing each of the voxel intensities separately:

$$P(Y|L,\Phi) = p(y_1|l_1,\Phi) * p(y_2|l_2,\Phi) .. * p(y_N|l_N,\Phi)$$

$$= \prod_{\forall j} p(y_j|l_j,\Phi)$$

What are the best parameter values?

On plausible definition: look for the parameter values Φ that maximize the likelihood of the observed image

$$\hat{\Phi} = \underset{\Phi}{\operatorname{argmax}}\, p(Y \mid L, \Phi)$$

Or preferably the log likelihood:

$$\hat{\Phi} = \underset{\Phi}{\operatorname{argmax}} \log_e p(Y \mid L, \Phi)$$

of the whole image:

$$\hat{\Phi} = \underset{\Phi}{\operatorname{argmax}} \log_e \prod_{\forall j} p(y_j \mid l_j, \Phi)$$

$$= \underset{\Phi}{\operatorname{argmax}} \sum_{\forall j} \log_e p(y_j \mid l_j, \Phi)$$

Maximizing Likelihood

$$\hat{\Phi} = \underset{\Phi}{\operatorname{argmax}} \sum_{\forall j} \log_e p(y_j \,|\, l_j, \Phi)$$

- Need to find:
  - The tissue label map L
  - The set of intensity model parameters Φ for each tissue class.

- No closed form solution available.

- BUT: Iterative EXPECTATION MAXIMIZATION (EM) algorithm is well suited for the case of a Gaussian Mixture Model. [Dempster et al., 1977]

->Labels are the 'missing data' to be estimated
MRI intensities are the observed data.

Expectation Maximization

$$\hat{\Phi} = \underset{\Phi}{\operatorname{argmax}} \sum_{\forall j} \log_e p(y_j | l_j, \Phi)$$

E

Expectation Evaluation Step

Given current intensity parameters:

$$\Phi = \{\mu_1, \sigma_1, c_1 ..... \mu_K, \sigma_K, c_K\}$$

Evaluate the expectation of label k at each voxel j

$$p_{jk}^{(m+1)} = \frac{G(y_j, \mu_k^{(m)}, \sigma_k^{(m)}) c_k^{(m)}}{\sum_{r=1}^{K} G(y_j, \mu_r^{(m)} \sigma_r^{(m)}) c_r^{(m)}}$$

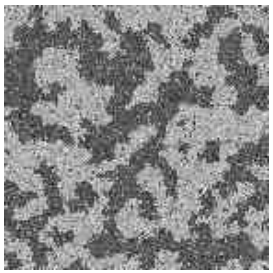

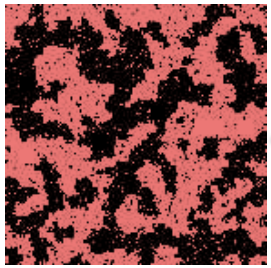

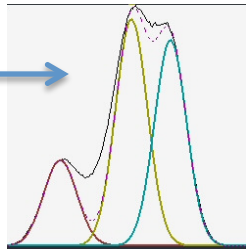

M

Maximization Step

Given current expectation of tissue labels at each voxel j

Find most likely values for intensity model parameters

$$\mu_k^{(m+1)} = \frac{\sum_{\forall j} y_j p_{jk}^{(m+1)}}{\sum_{\forall j} p_{jk}^{(m+1)}}$$

$$(\sigma_k^{(m+1)})^2 = \frac{\sum_{\forall j} (y_j - \mu_k^{(m+1)})^2 p_{jk}^{(m+1)}}{\sum_{\forall j}^{n} p_{jk}^{(m+1)}}$$

$$c_k^{(m+1)} = \frac{1}{n} \sum_{\forall j} p_{jk}^{(m+1)}$$

T1W MRI Brain Tissue Labeling

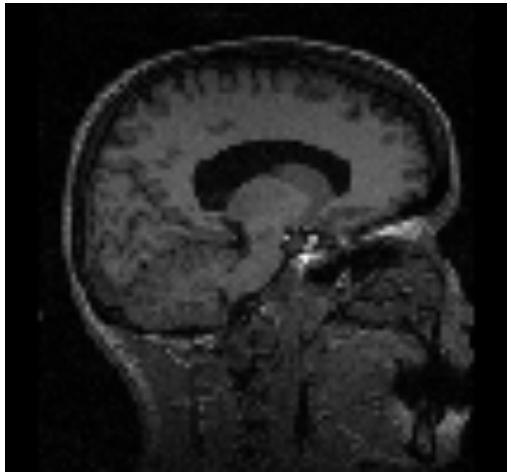

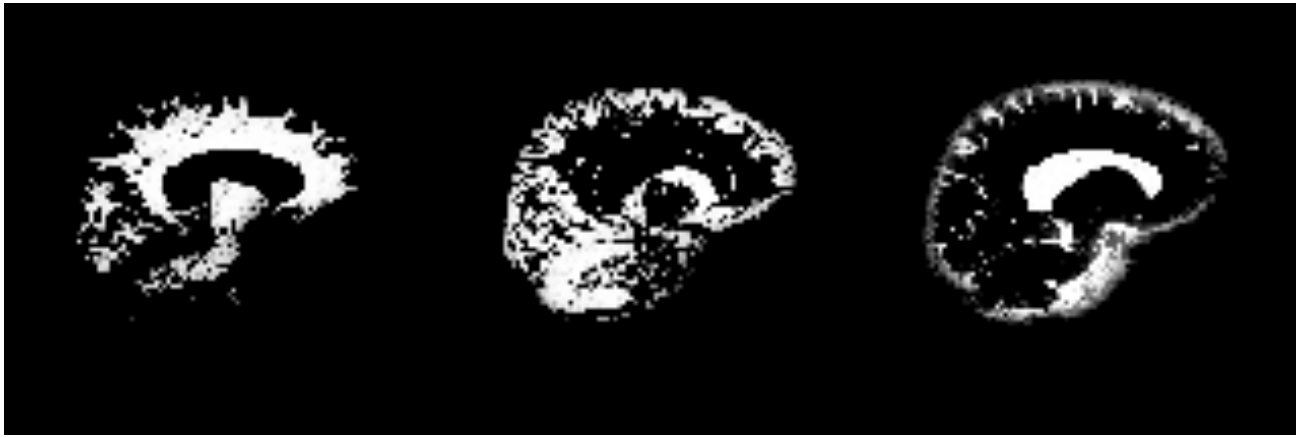

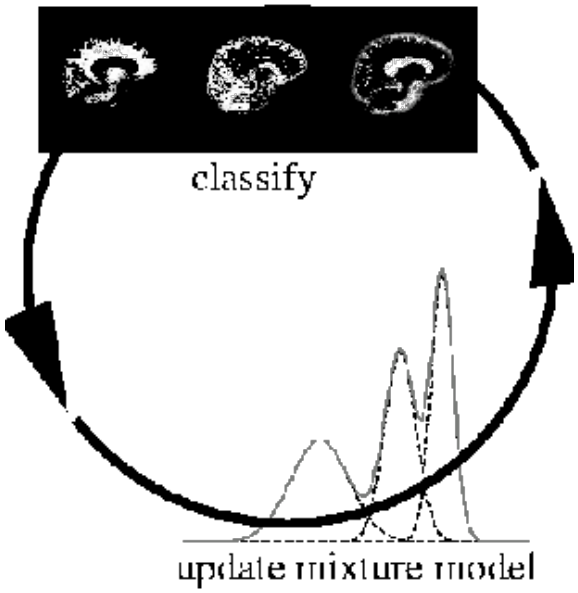

Simultaneous classification and parameter estimation

Likelihood is guaranteed to increase at each iteration

The need for Prior Information

- The EM algorithm provides only a LOCAL optimum
  - It is highly dependent on starting estimate
- Tissue type is not completely explained by image intensity
  - need spatial context.
  - How to initialize algorithm with intensity parameters or labels?

Atlas Based Priors:
A spatial model of brain tissues

- Constructed by taking many example segmented brains:
  mapped to a reference anatomy using non-rigid registration

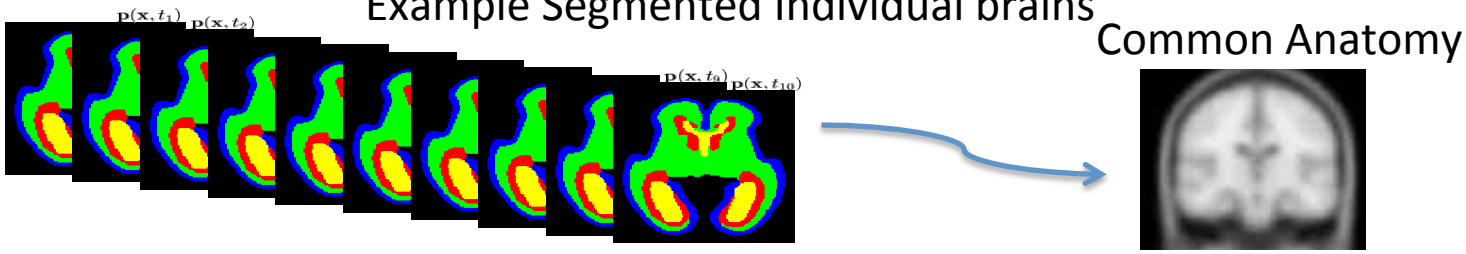

- Form an AVERAGE to capture the expected location
  of major tissue types in the population used.

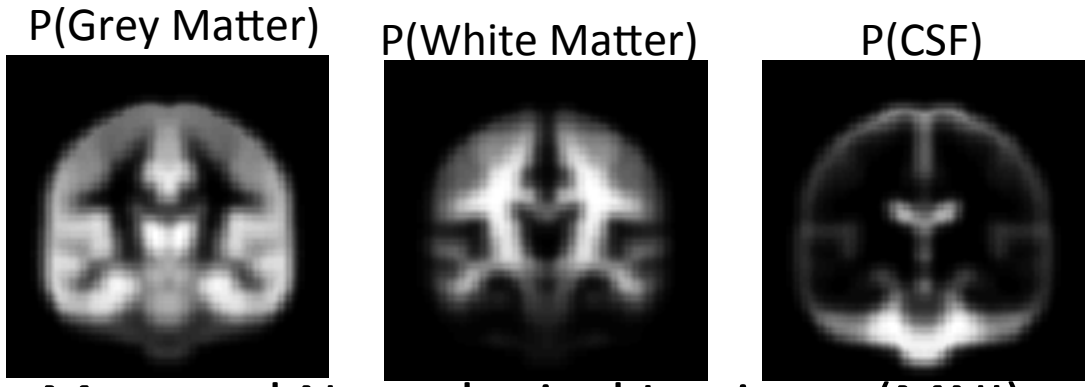

- Example: Montreal Neurological Institute (MNI) atlases

Automated Segmentation of New subject MRI: Mapping Atlas Priors to Subject Anatomy

Average MRI of Atlas Data

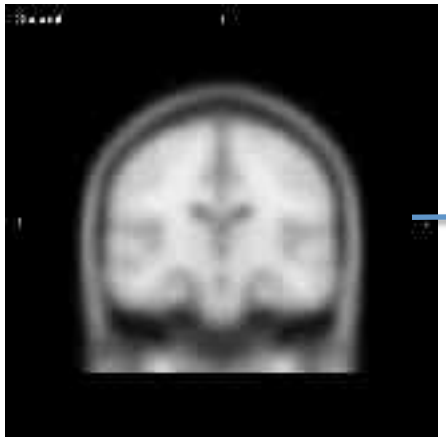

Average MRI of Atlas Data in Subject Space

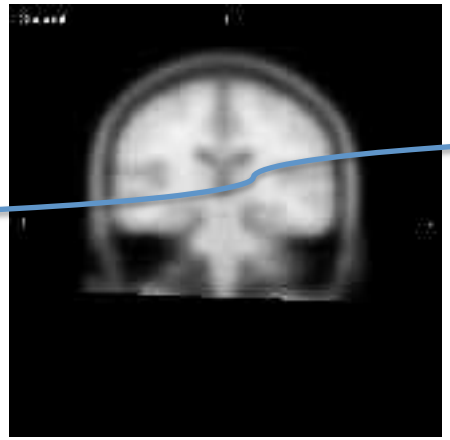

MRI of new Subject

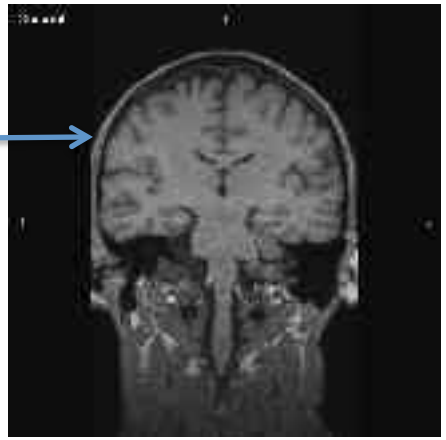

White Matter Probability

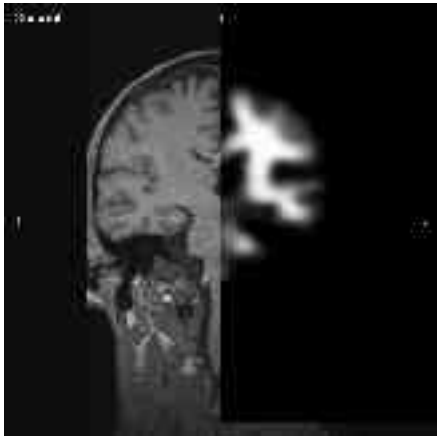

Grey Matter Probability

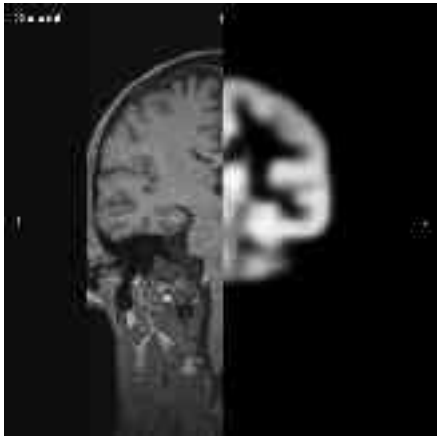

Cerebrospinal fluid probability

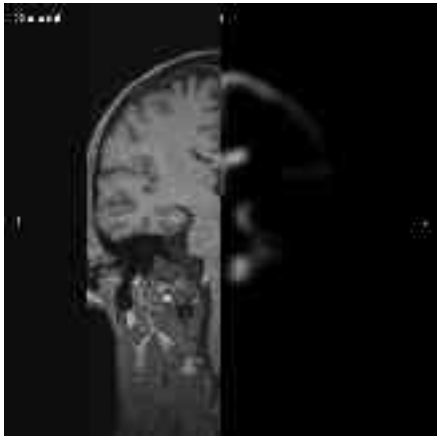

Using Spatial Priors in EM labeling

$$\hat{\Phi} = \underset{\Phi}{\operatorname{argmax}} \sum_{\forall j} \log_e p(y_j | l_j, \Phi)$$

E Expectation Evaluation Step

Expectation of label k at each voxel j
given current estimate
for intensity model parameters
Moderated by Spatially Varying Atlas Priors

[Ashburner and Friston, 1997]

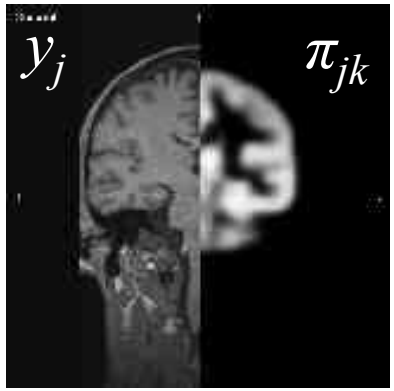

$$p_{jk}^{(m+1)} = \frac{G(y_j, \mu_k^{(m)}, \sigma_k^{(m)}) c_k^{(m)} \pi_{jk}^{(m)}}{\sum_{r=1}^{K} G(y_j, \mu_r^{(m)} \sigma_r^{(m)}) c_r^{(m)} \pi_{jr}^{(m)}}$$

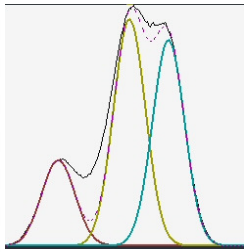

M Maximization Step

Most likely values for intensity model parameters, given labels

$$\mu_k^{(m+1)} = \frac{\sum_{\forall j} y_j p_{jk}^{(m+1)}}{\sum_{\forall j} p_{jk}^{(m+1)}}$$

$$(\sigma_k^{(m+1)})^2 = \frac{\sum_{\forall j} (y_j - \mu_k^{(m+1)})^2 p_{jk}^{(m+1)}}{\sum_{\forall j}^{n} p_{jk}^{(m+1)}}$$

$$c_k^{(m+1)} = \frac{1}{n} \sum_{\forall j} p_{jk}^{(m+1)}$$

Further Development of Brain Tissue Segmentation Methods

- Bias Field Estimation:
  - Tissue signal is spatially varying
    (like an illumination model for MRI).
    - Fit a smoothly varying multiplicative field to each class.
  - [eg: Wells et al, TMI 1996; Guillemaud and Brady TMI 1997]

- Partial volume effect:
  - voxels at boundaries contain contributions for different tissue classes
  - Need to Model compartmental contributions to voxel intensity
    - [eg: Shattuck et al, Neuroimage 2000; Ballester 2002;
      Choi, H. S., Haynor, D. R., and Kim, Y. TMI 1991.]
- Smoothness priors to remove single voxel errors:
  - Give neighbors an influence on each other
    - Markov Random Field

Developments of EM segmentations: Limitations of Priors

- Variations in anatomy that cannot be directly parameterized:
  - Brain tumor (space occupying)
  - Brain injury (eg blood clot)
  - Surgical resection/implants

  [Van Leemput et al., TMI 2001, Zijdenbos TMI 1994]

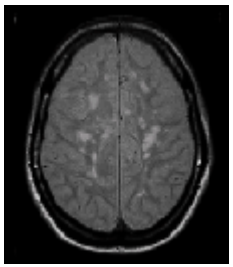

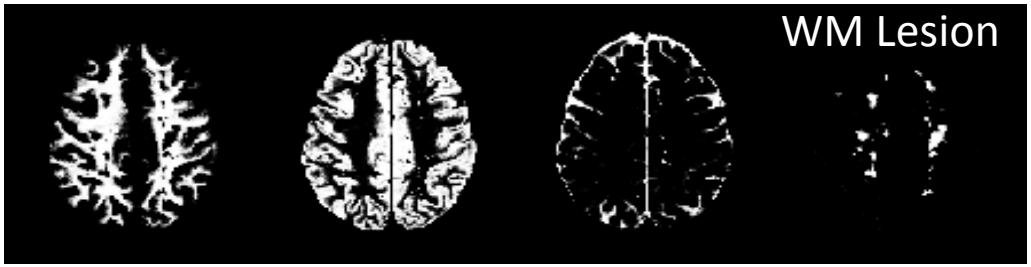

- Variations that can be parameterized:
  - Age: in the study of the growing brain

  [Habas et al Neuroimage 2010]
- Alternative Geometries for Tissue Statistics:
  - Layers in the fetal brain
  - [Habas et al Proc. SPIE Medical Imaging, 2009]

A motivation for new work: Fetal Brain MR imaging

- Clinical evaluation of pregnancy
- Early identification of brain abnormalities
- Detects tissue boundaries invisible on ultrasound
- Essential for the study of normal and abnormal brain development in utero

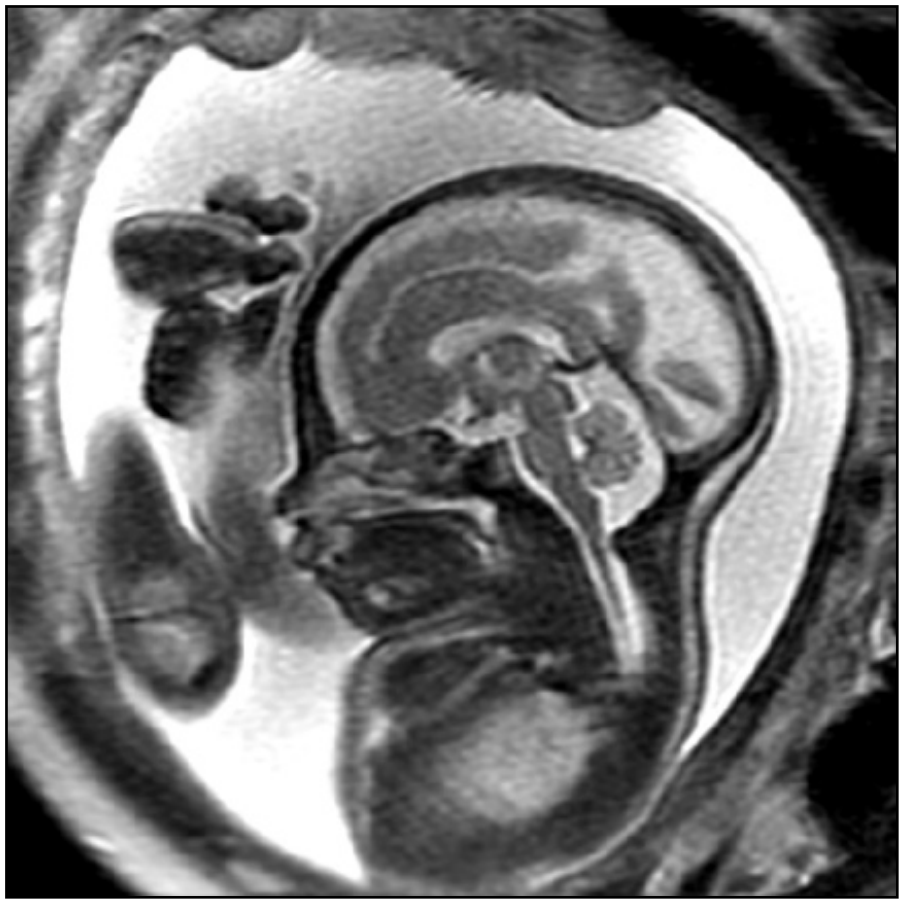

Example Clinical Images

- **T2W Multi Slice**
  - Single shot fast spin echo (SSFSE; 2D)
  - T2 weighted
  - TR = 4500 ms, TE = 90 ms
  - Approximately 1x1x3 mm^3 voxel dimension
  - 15~30 slices in each stack
- **Anisotropic resolution with thick slices**
- **Often Acquired using Real Time Planning tools**

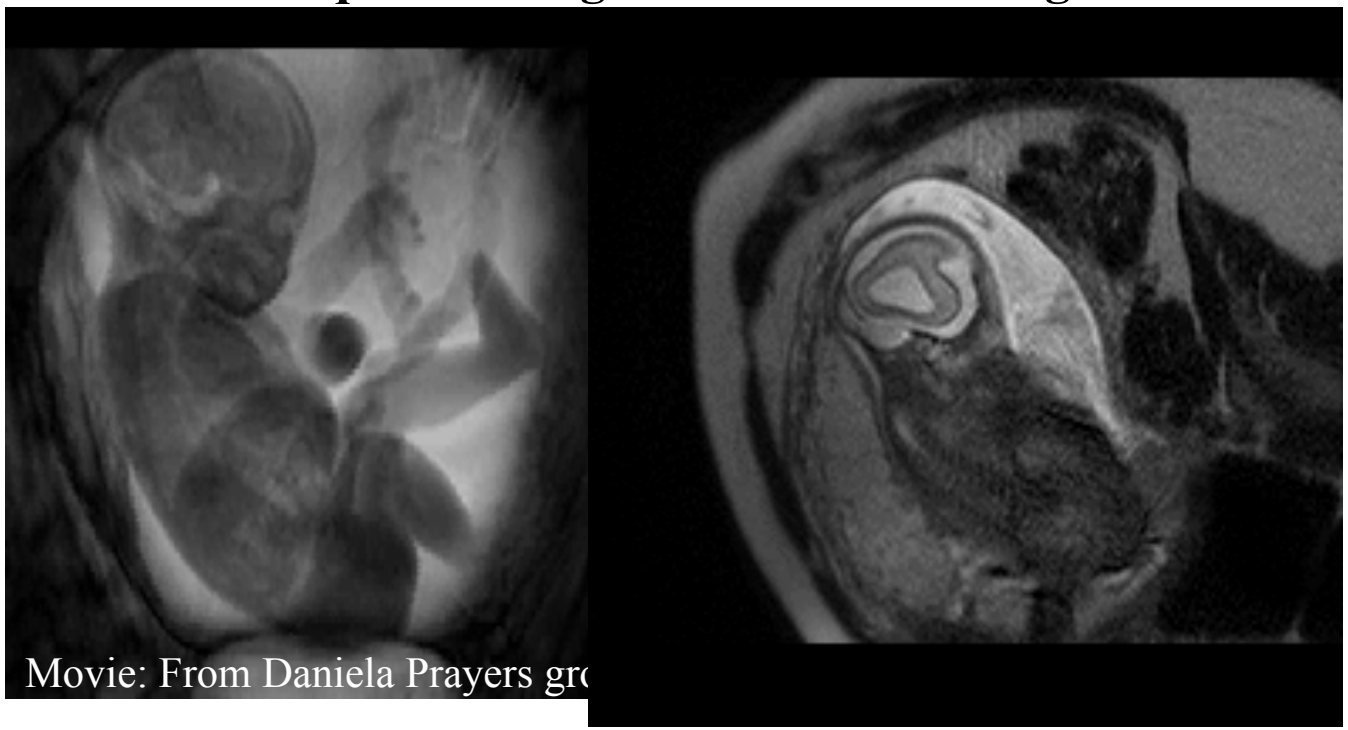

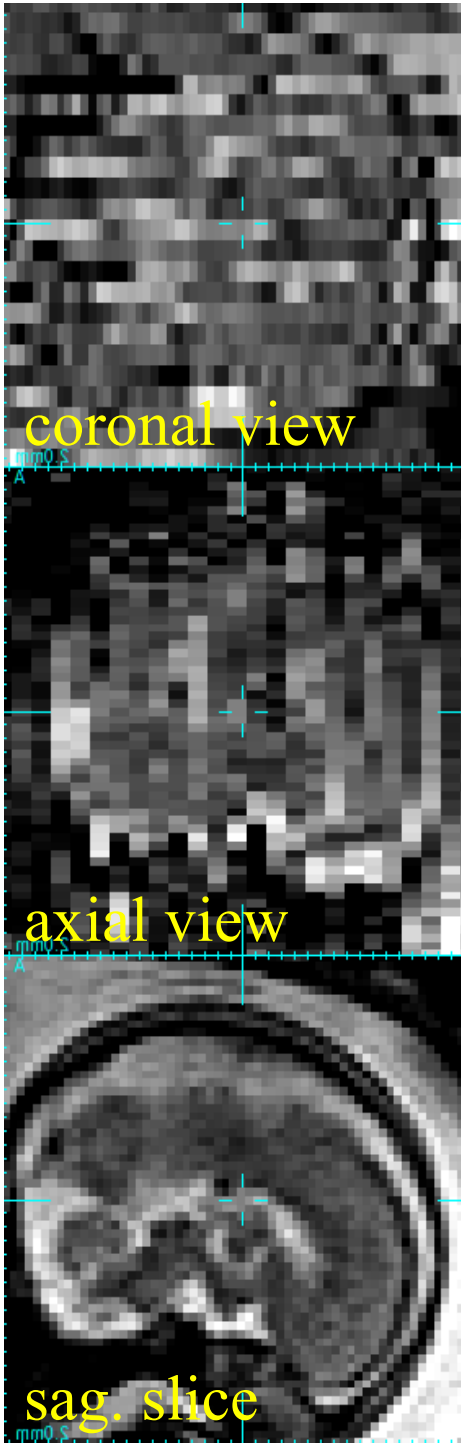

Fetal MRI reconstruction

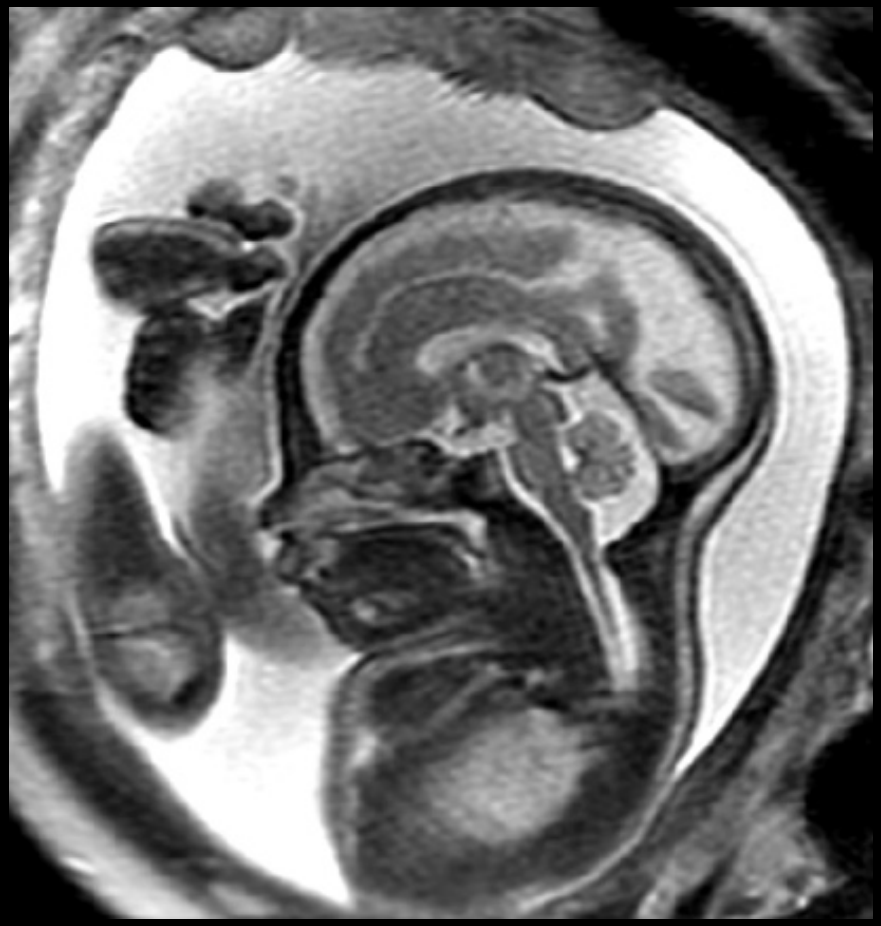

Rousseau et al, Academic Radiology 2006.

Kim et al., "Intersection-based motion correction of multi-slice MRI for 3D in utero fetal brain image formation," IEEE Transactions on Medical Imaging, TMI 2010

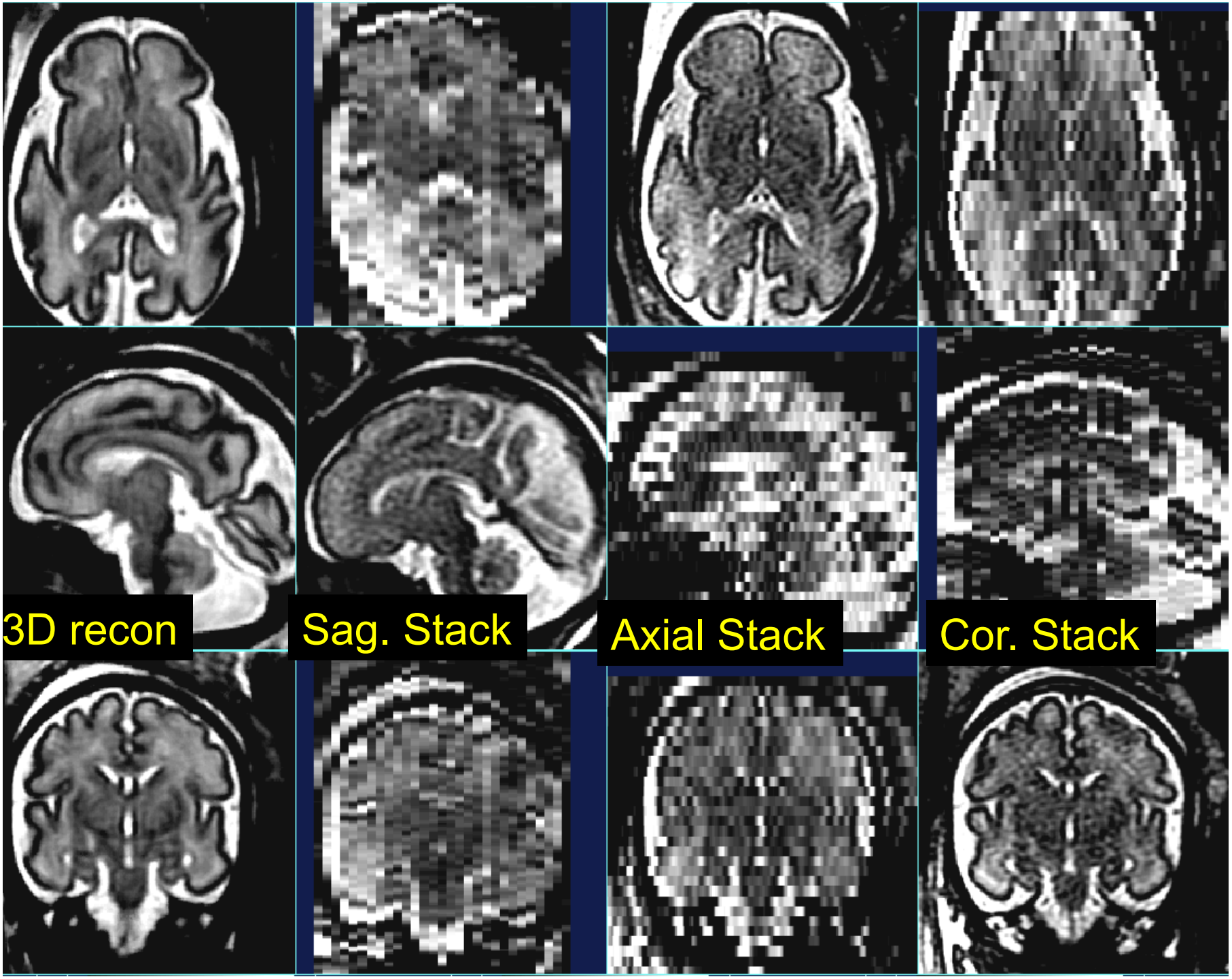
3D recon
Sag. Stack
Axial Stack
Cor. Stack

Challenges in fetal brain MRI Analysis

- adult brain analysis methods cannot be directly applied
  - different geometry
  - different tissue morphology
- Rapid changes occurring over very short time:
  - shape/size changes
  - intensity/contrast changes
  - appearance and disappearance of transient tissue types from different brain regions
- Underlying anatomy must be interpreted in relation to its developmental stage

T2W Fetal MRI

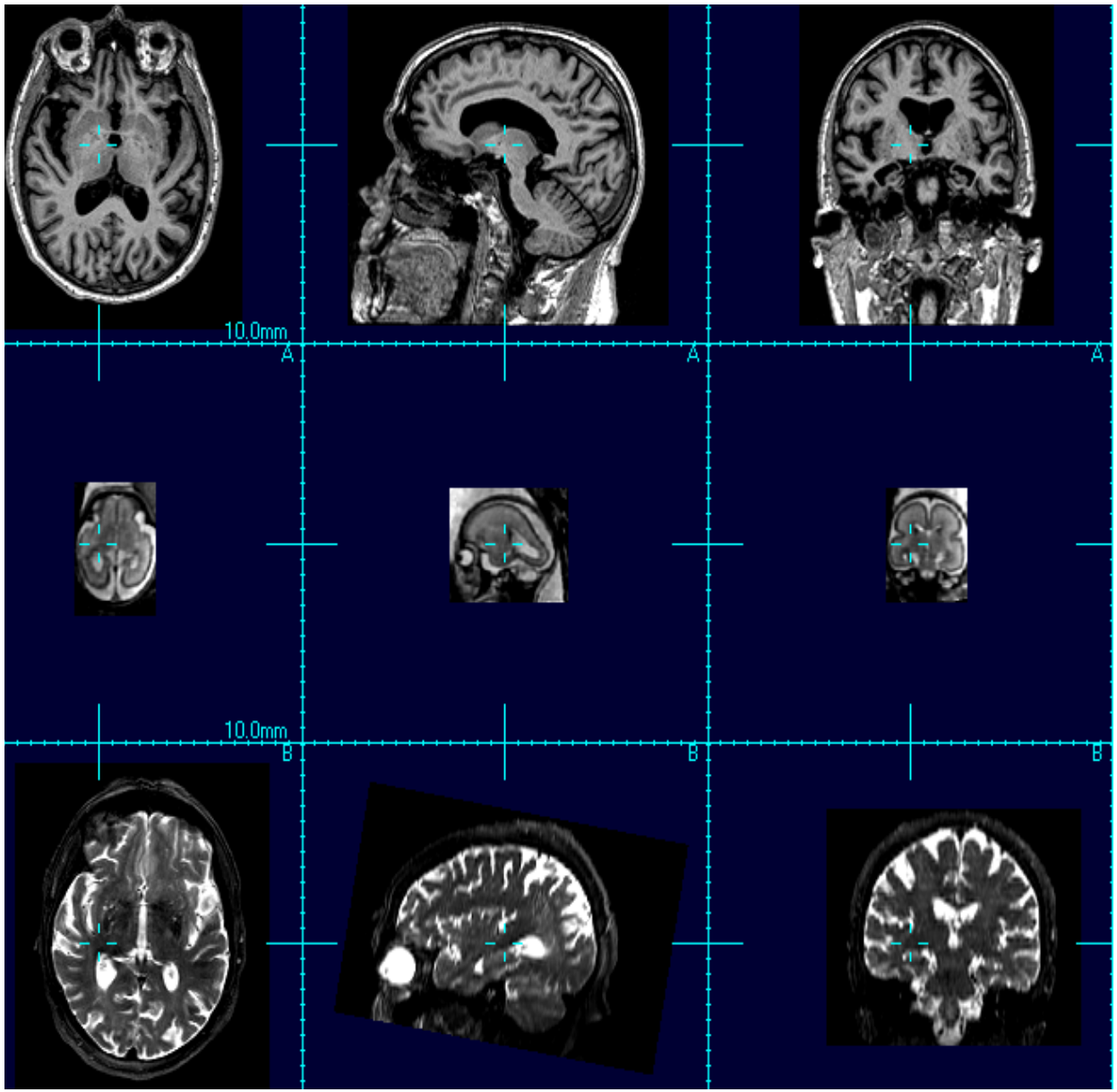

T1W Adult

T2W Fetus
Approx 22W GA

T2W Adult

Fetal Brain Tissue Zones

Cortical Plate (CP)

Subplate (SP)

Intermediate Zone (IZ)

Germinal Matrix (GMAT)

-> Peri Ventricluar Zone
+Sub Ventricular Zone

Ventricular CSF (VENT)

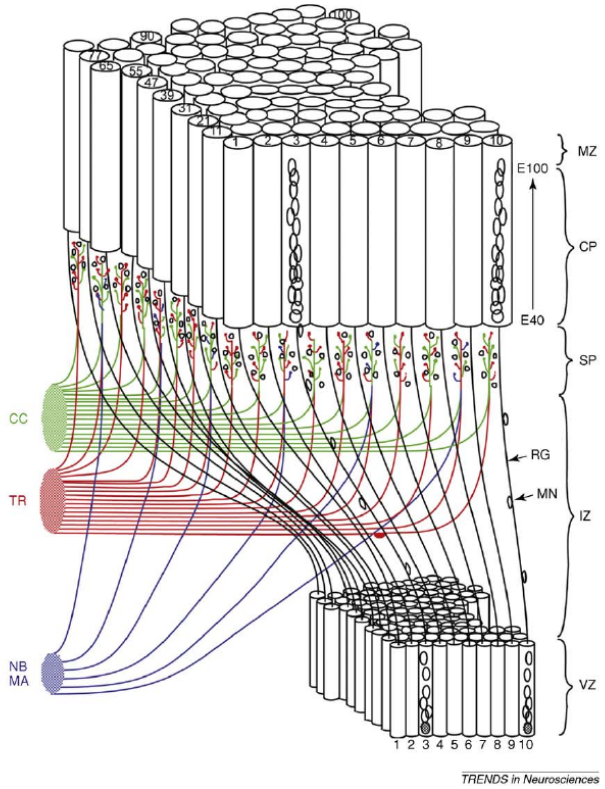

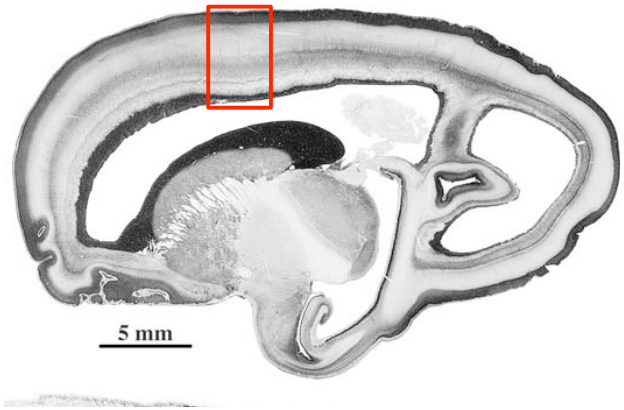

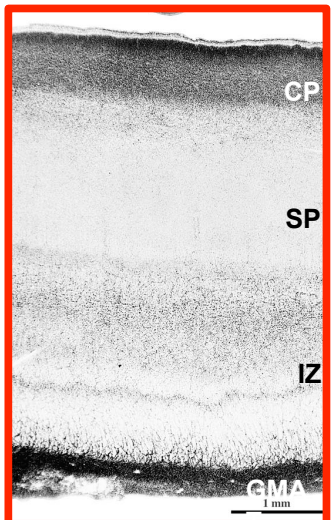

Laminar organization of the fetal brain

T1W MRI (Pathology)

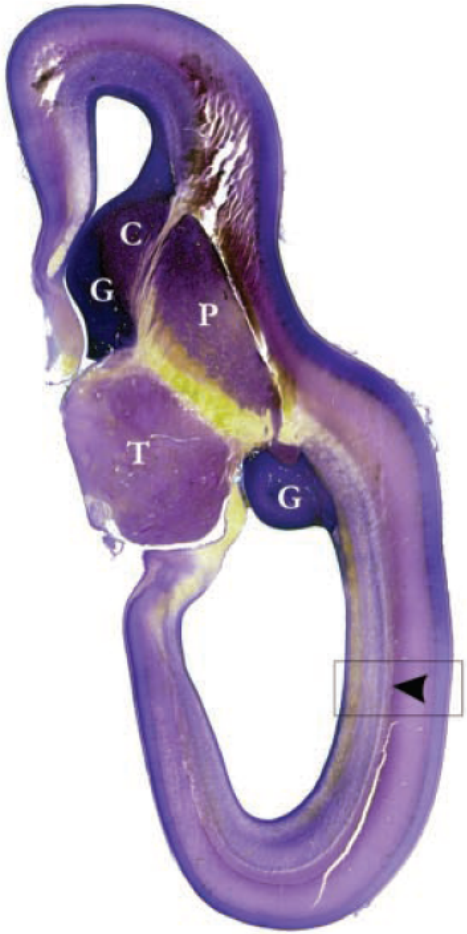

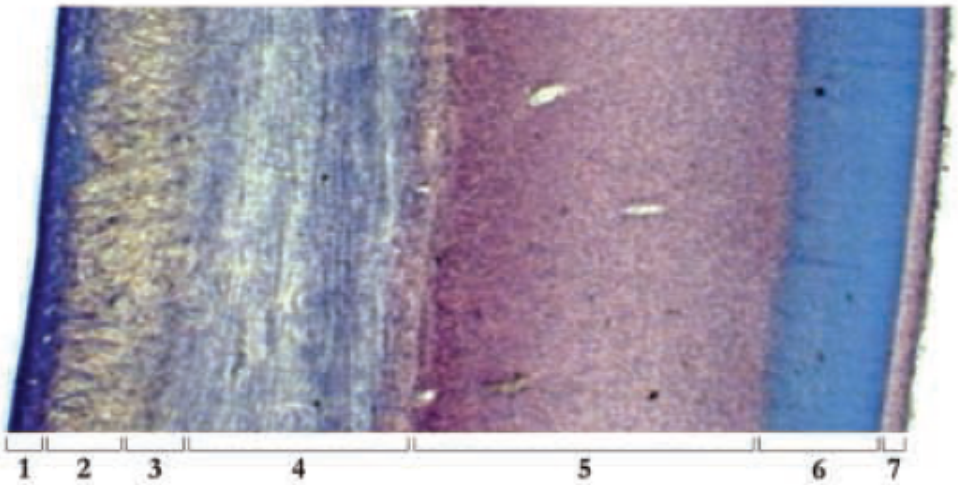

1 = Ventricular zone (germinal matrix)
2 = Periventricular fibre rich zone
3 = Subventricular cellular zone
4 = Intermediate zone (fetal "white" matter)
5 = Subplate zone
6 = Cortical plate
7 = Marginal zone

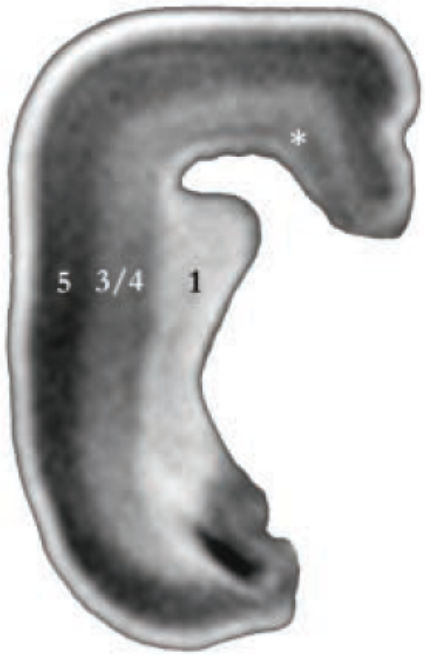

[Kostovic et al, Cerebral Cortex, 2002, 536-544]

Adult Brain tissue segmentation: Gaussian Mixture Model of Tissues

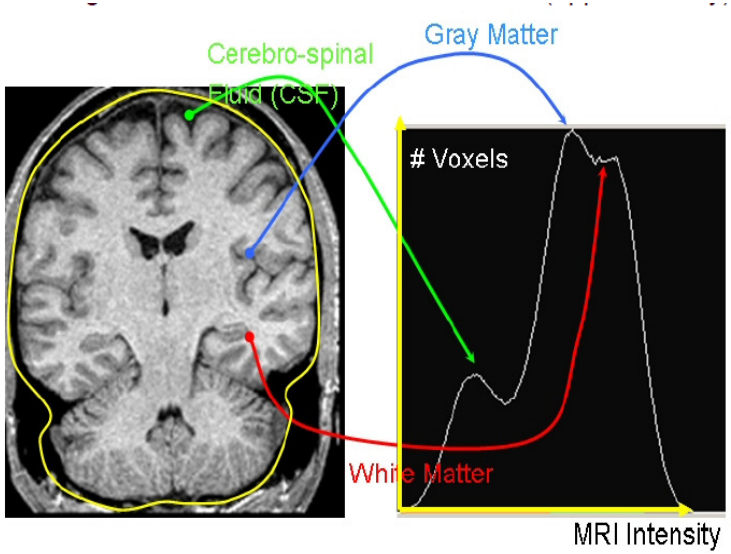

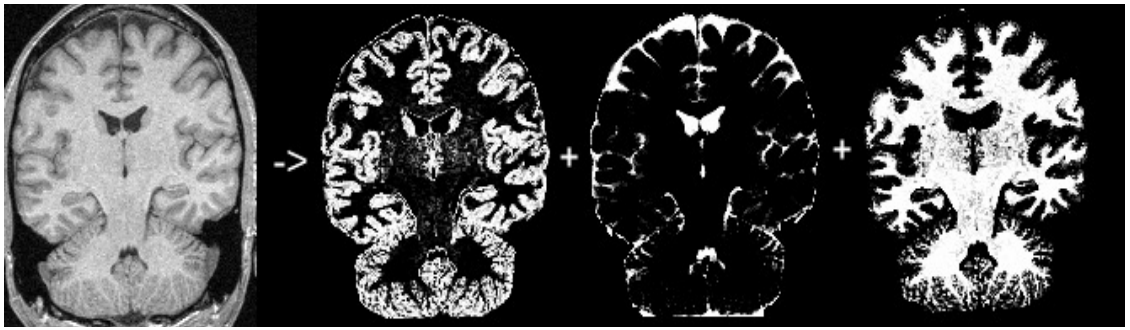

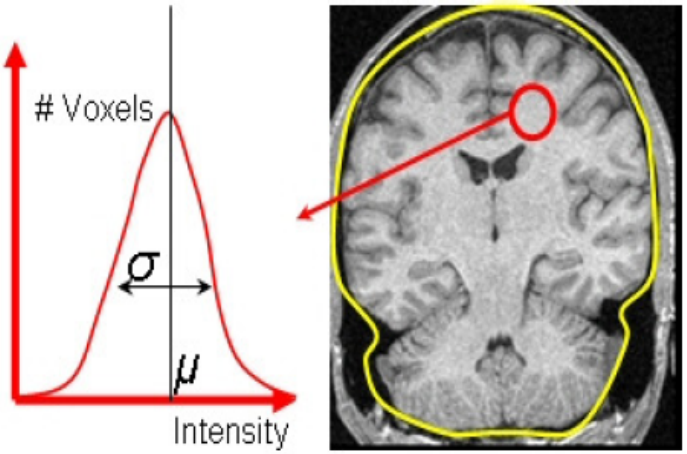

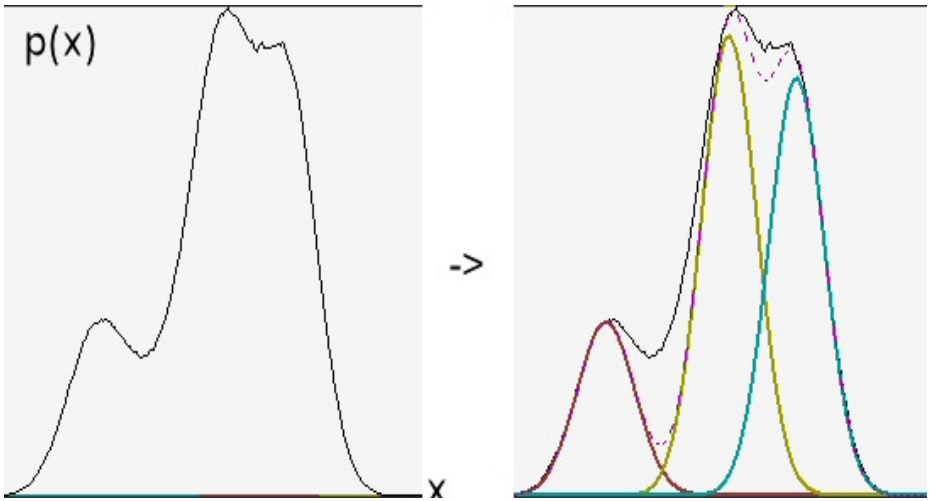

Challenges in fetal brain segmentation

- Adult brain analysis methods cannot be directly applied
  - different geometry
  - different tissue morphology

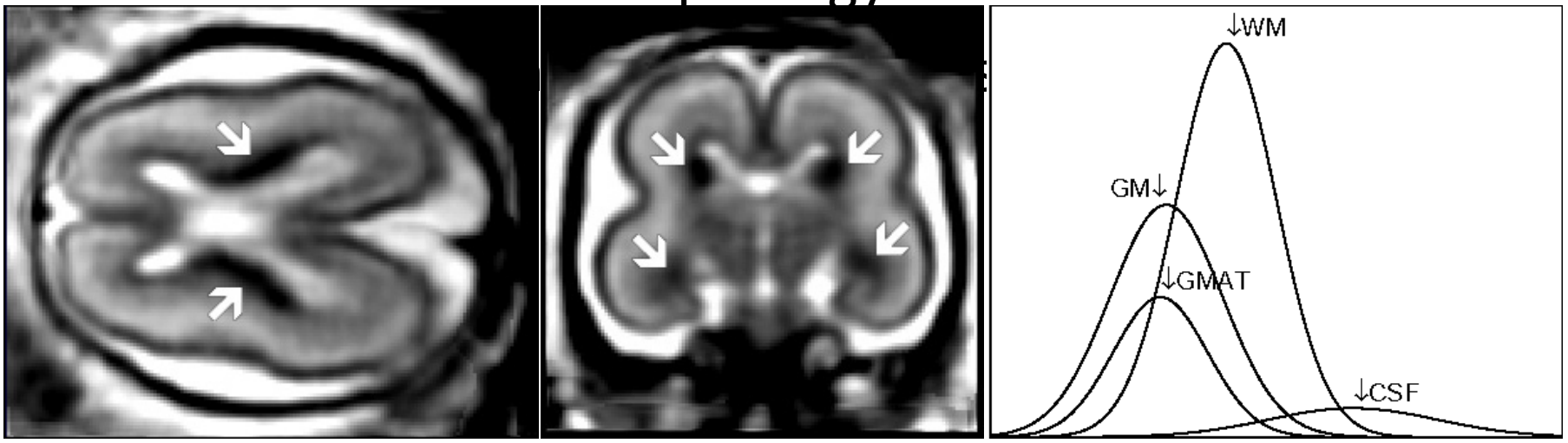

Habas et al., "Atlas-based segmentation of the germinal matrix from in utero clinical MRI of the fetal brain", Medical Image Computing and Computer Assisted Intervention, LNCS, vol. 5241, pp. 351-358, September 2008.

Fetal Atlas-based EM segmentation

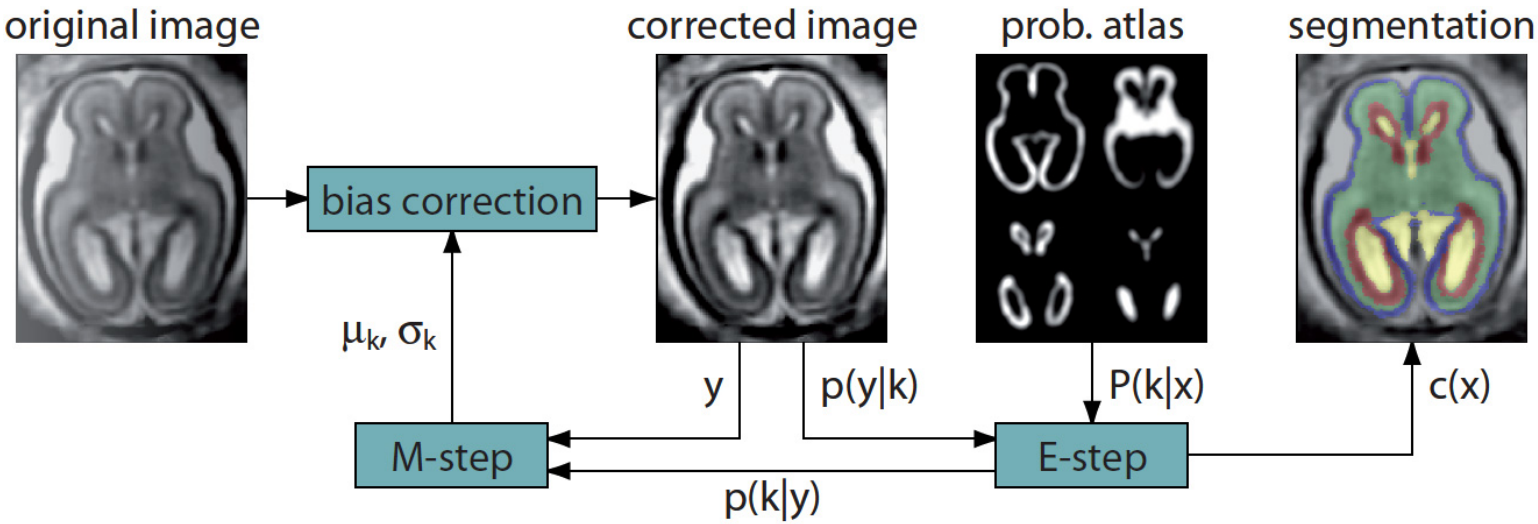

Need to make priors match subject anatomy in terms of gestational age (Weeks)

Habas et al.,Human Brain Mapping 2010.

Building a Spatiotemporal atlas of the fetal brain

- Use of age-specific atlases can improve results of automated brain image analysis
- BUT: Separate atlases needed for different weeks of fetal brain development
- BETTER approach: a 4D or parameterized atlas of tissue distribution:
  - temporally parameterized tissue probabilities for each voxel
- Multiple timepoint imaging of same fetus not feasible

Statistical Model of Developing Tissue Distribution

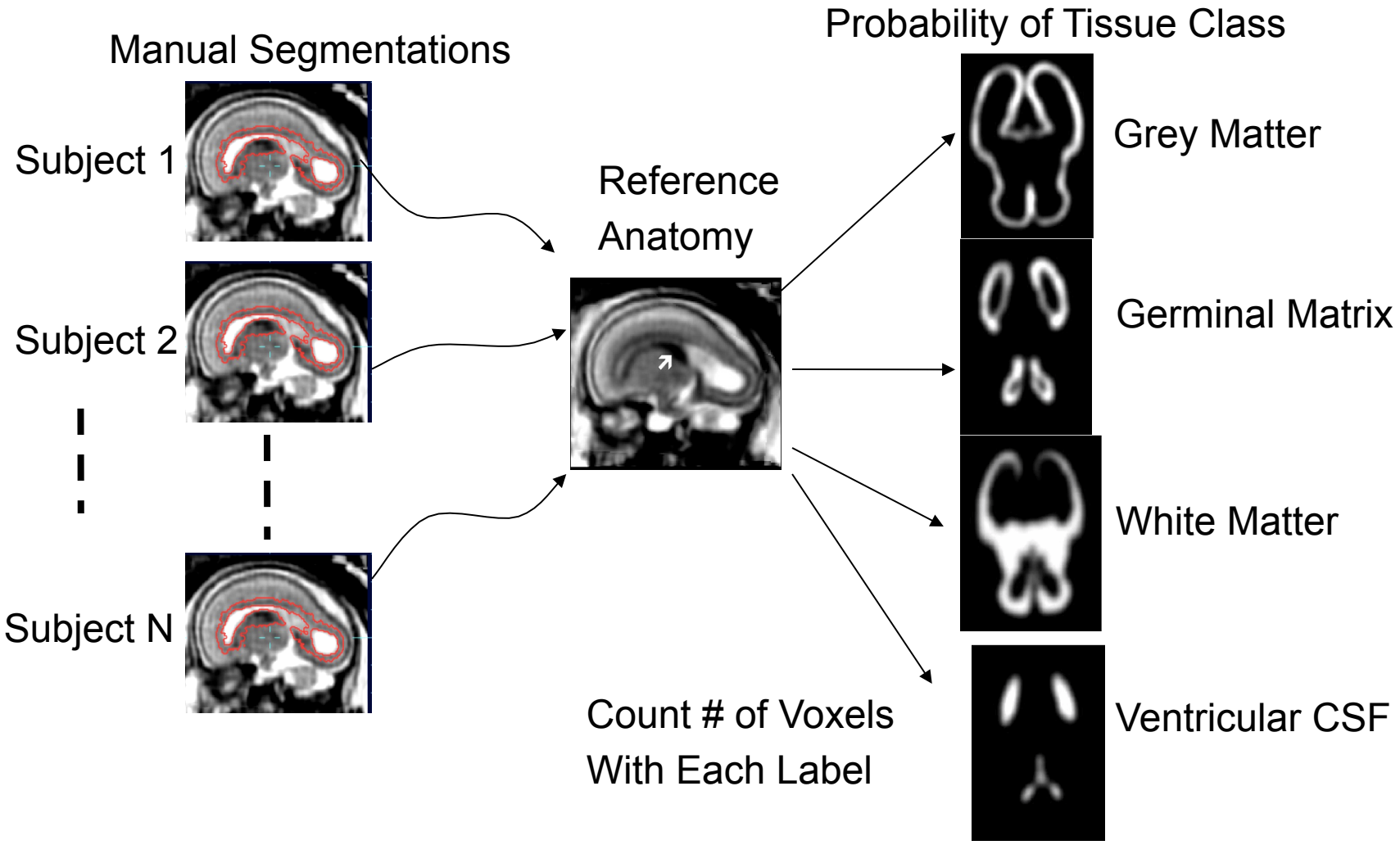

Voxelwise modeling from registered maps

Given eample tissue segmentations from different ages placed into common anatomical space

Assume: each voxel in common anatomy has tissue probability which varies with time

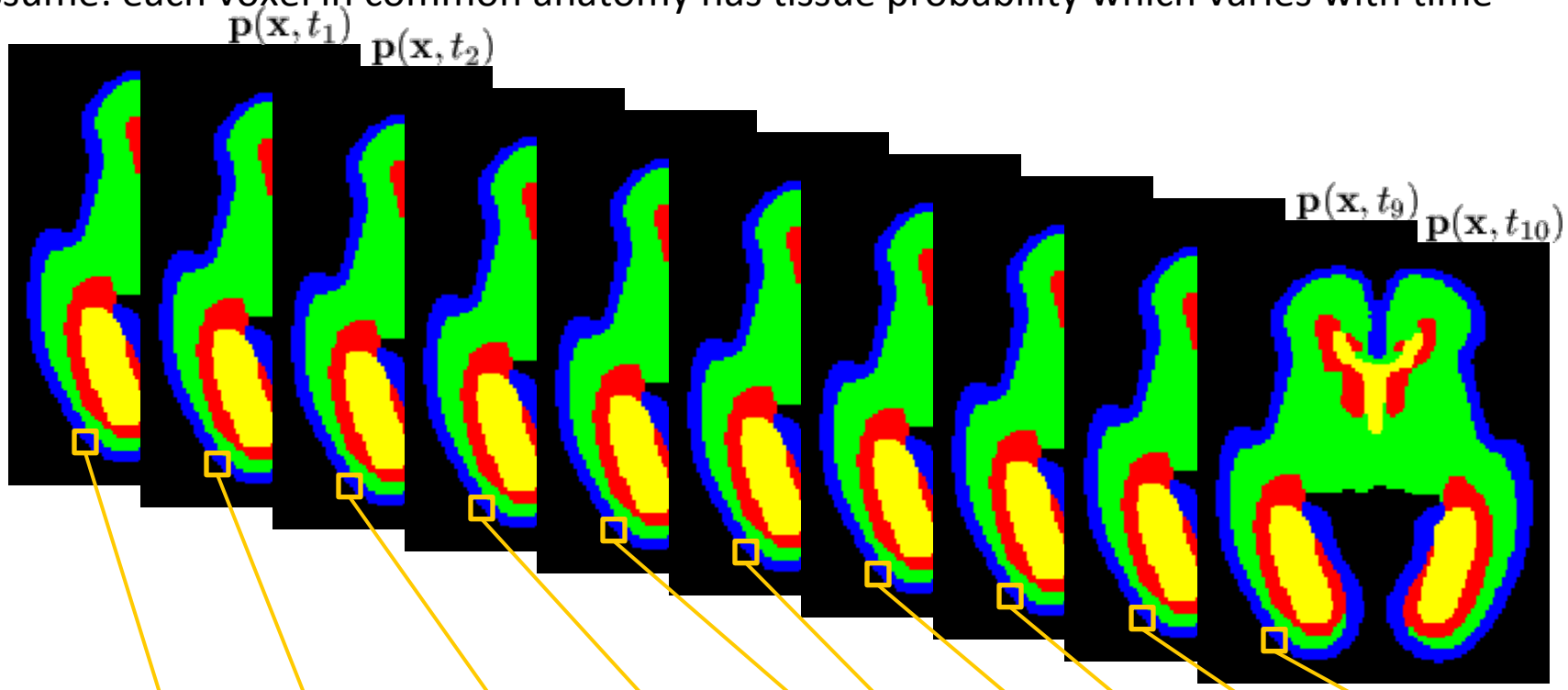

Consider one Voxel, two tissue classes, binary segmentations (0 or 1):

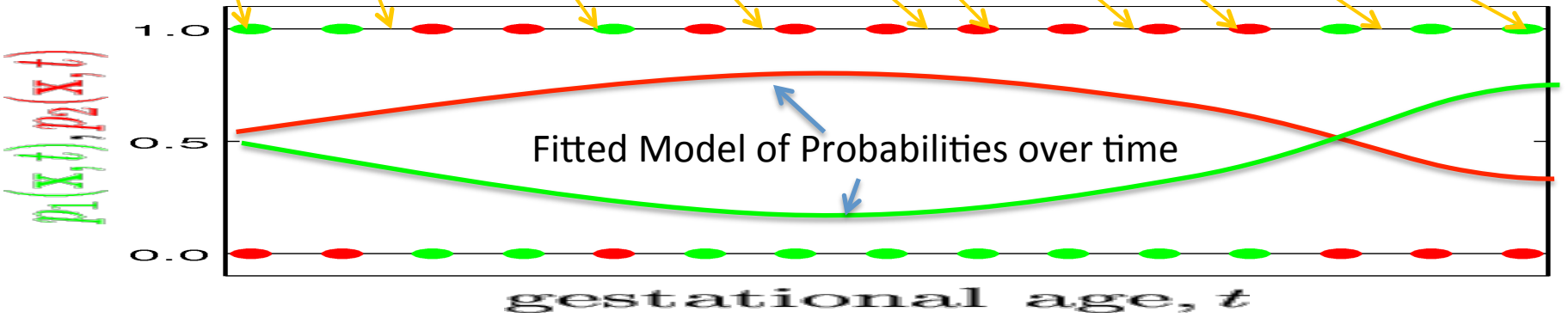

Temporal modeling of tissue probabilities

Could use a simple polynomial model of probability change with time
So that probability of a tissue class k at voxel j, for a given time t is:

$$p_{jk}(t) = \sum_{d=0..D} a_{jkd} t^d$$

where a_{jkd} are a set of coefficients fitted to the data points at voxel k

eg a quadratic model (D=2) to capture a peak of tissue probability in time:

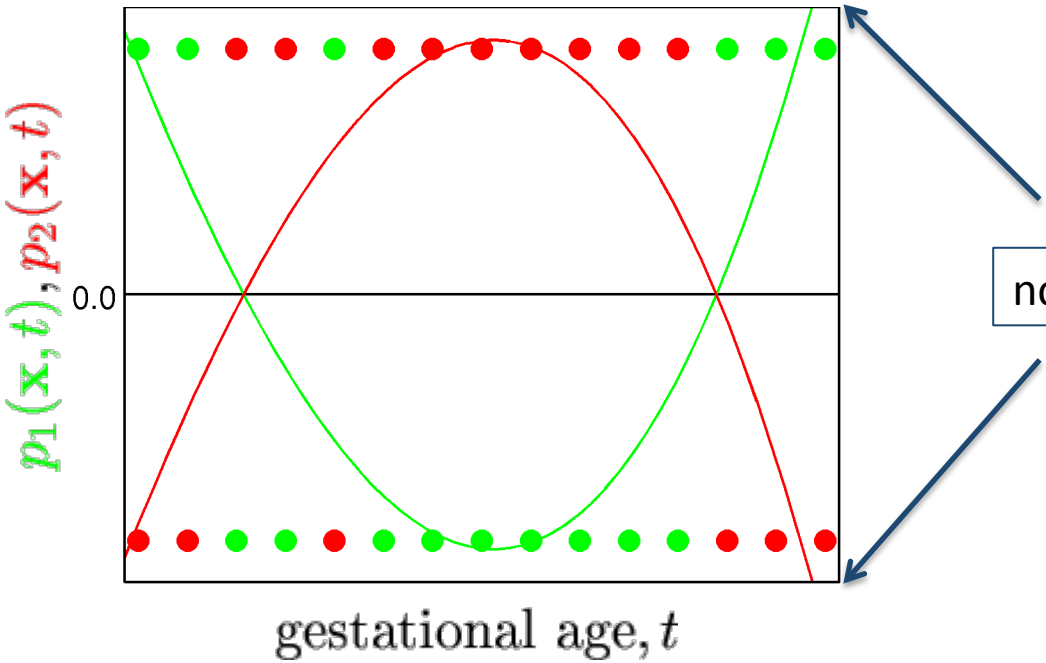

not a probability!

Problem:
Model not constrained within the space of probabilities (0..1)

Solution: LogOdds Temporal modeling of tissue probabilities

LogOdds transform maps between [0..1] <-> scalars

$$\mathcal{L}(p_k(\mathbf{x},t)) = \log\left(\frac{p_k(\mathbf{x},t)}{1-p_k(\mathbf{x},t)}\right) = l_k(\mathbf{x},t)$$

Fit model in LogOdds space

$$l_{jk}(t) = \sum_{d=0..D} a_{jkd} t^d$$

probability space

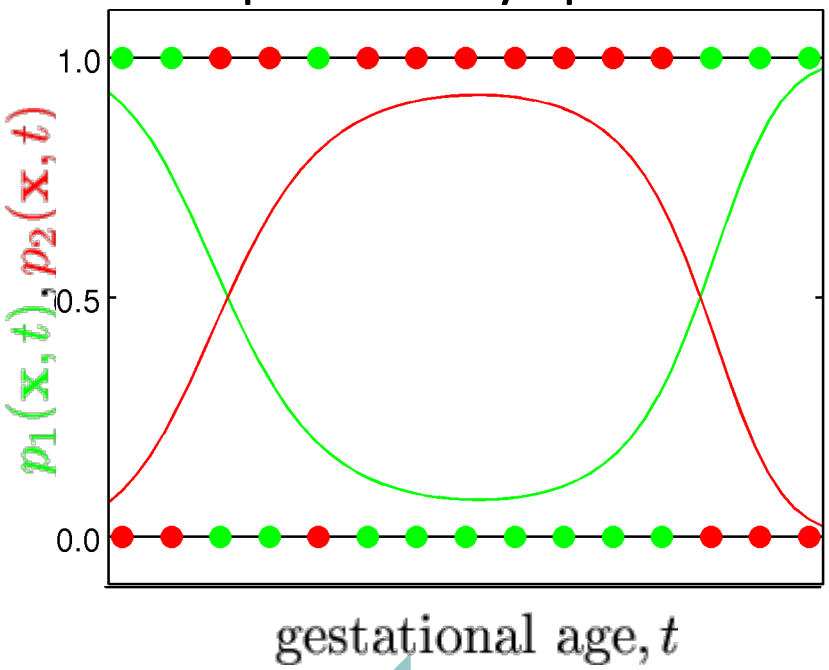

LogOdds space

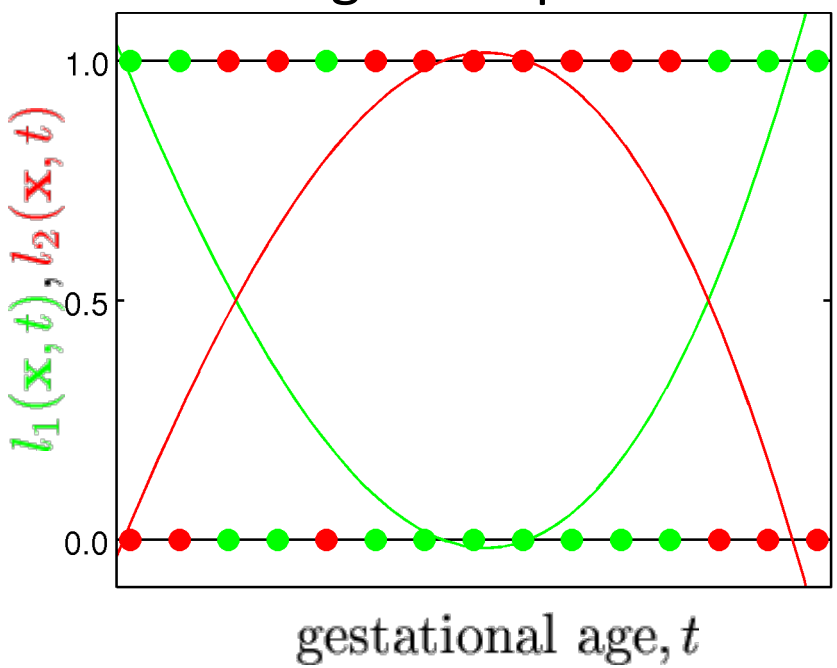

$$\mathcal{L}^{-1}(l_k(\mathbf{x},t)) = \frac{1}{1+\exp(-l_k(\mathbf{x},t))} = p_k(\mathbf{x},t)$$

Pohl et al., "Logarithm odds maps for shape representation", Medical Image Computing and Computer Assisted Intervention, LNCS, vol. 4191, 2006.

No temporal dependency ($D = 0$)

- Equivalent to conventional averaging of spatially normalized tissue label maps
- Affected by age distribution within subject group

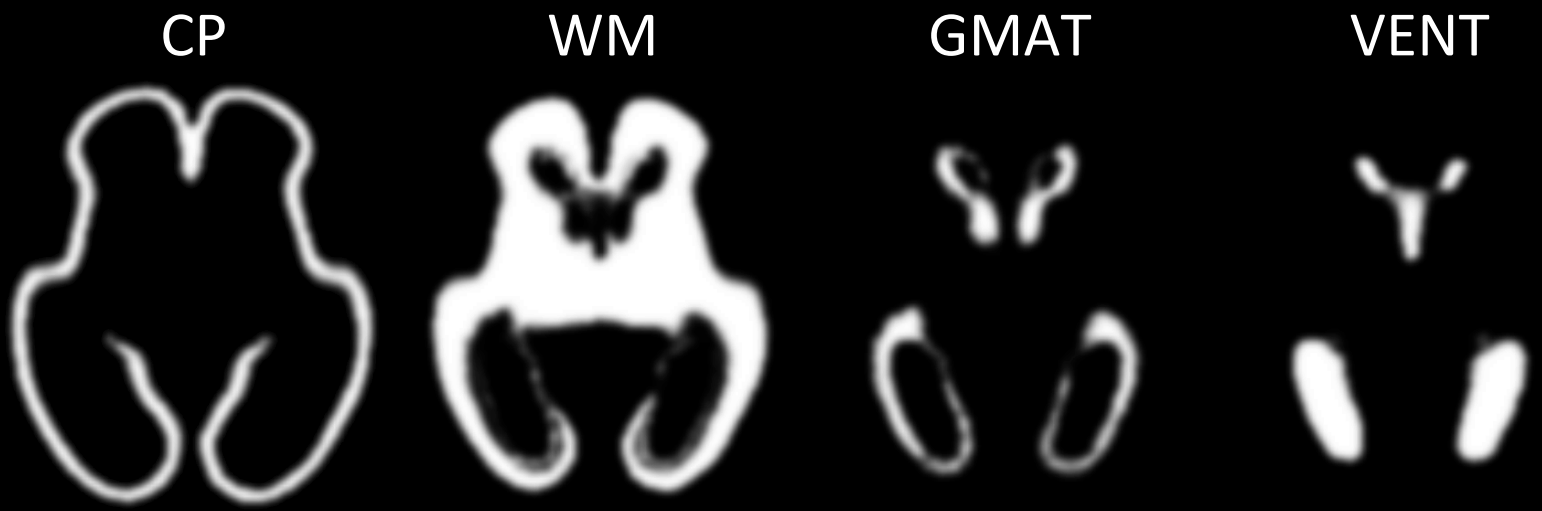

Tissue probability maps generated in average space

Quadratic temporal model ($D = 2$)

Age-specific tissue probability maps generated in average space

Automated Fetal Tissue Segmentation

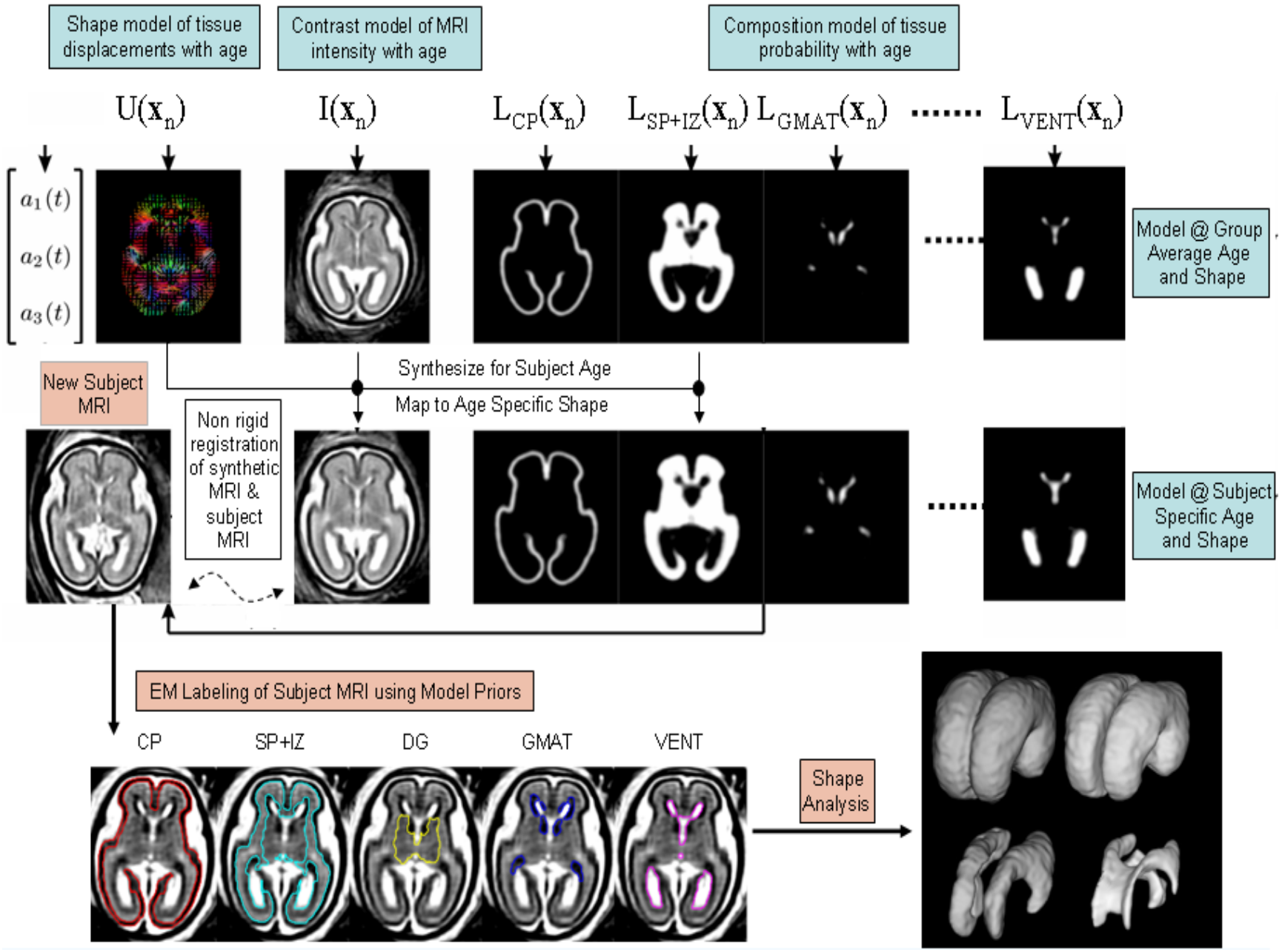

Resolving temporal correspondence

- Challenge:
  - we need to define consistent mapping between subject anatomies with different ages
  - inconsistent structural features over time, e.g., appearance and disappearance of GMAT
  - can induce artefactually large deformations in non-rigid registration
- Approach:
  - exclude temporally inconsistent tissue boundaries
  - use only GM, WM+GMAT, and others (CSF, non-brain)

Fetal MR T2w imaging data

- 1.5T scanner, TR = 4000-8000 ms, TE = 91 ms, 0.5 mm x 0.5 mm in plane, 3 mm slice thickness
- Reconstructed into 3D volumes using SIMC

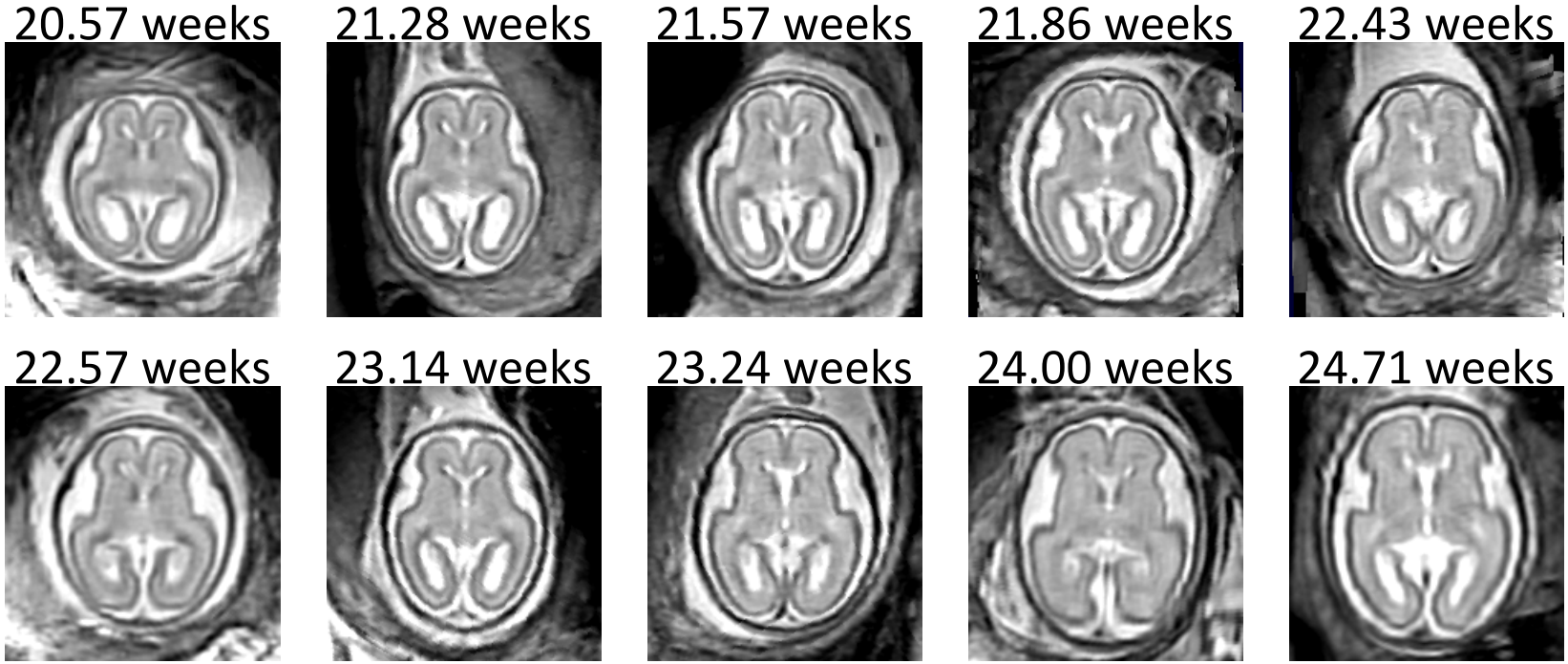

Results: Validation of atlas-based segmentation

- Single probabilistic atlas with D = 0 (constant avg)
- Age-specific probabilistic atlases generated for each subject with $D = 1$ and $D = 2$
- Atlas-based EM segmentations in subject space

Tissue or structure	$D = 0$	$D = 1$		$D = 2$	
	Average DSC	Average DSC	p	Average DSC	p
VENT	0.857±0.040	0.862±0.029	0.411	0.867±0.029	0.099
CP	0.834±0.014	0.835±0.013	0.168	0.836±0.013	0.180
WM	0.905±0.012	0.917±0.014	0.038	0.918±0.014	0.034
GMAT	0.642±0.131	0.752±0.069	0.012	0.761±0.081	0.011

3D fetal MRI segmentation

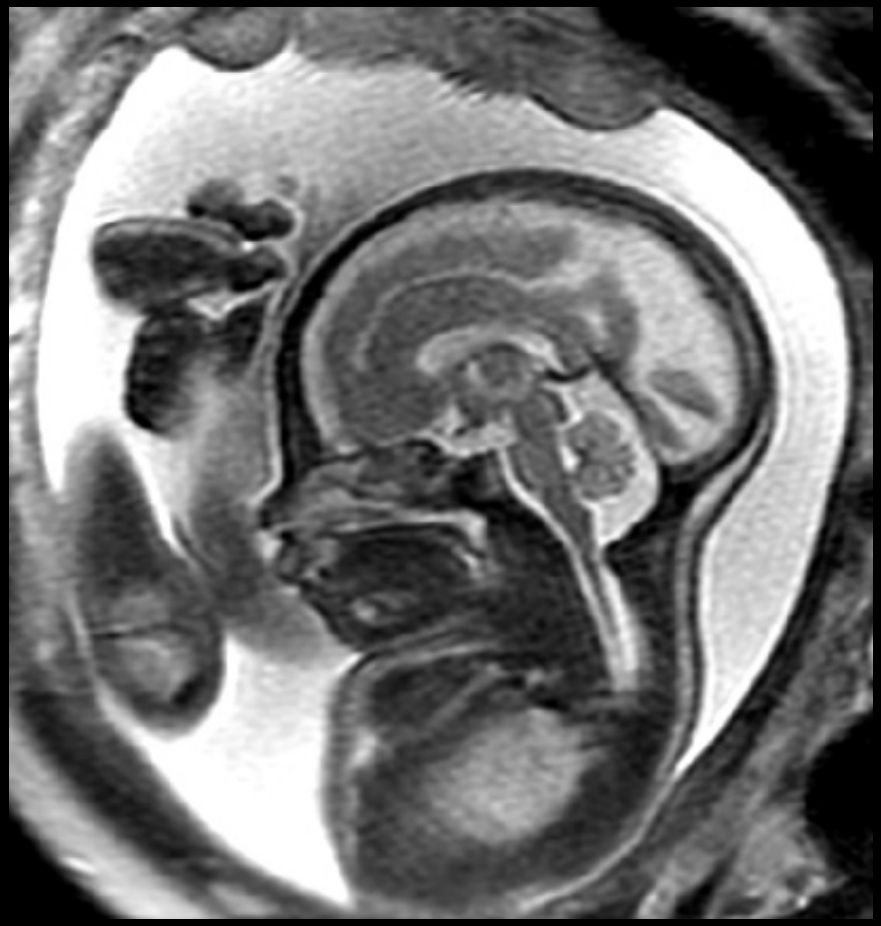

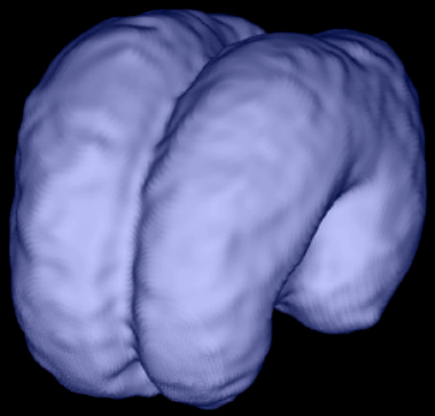

GM

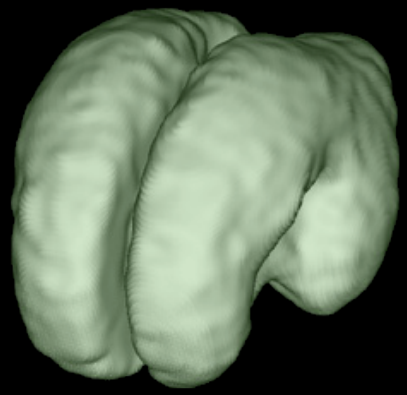

WM

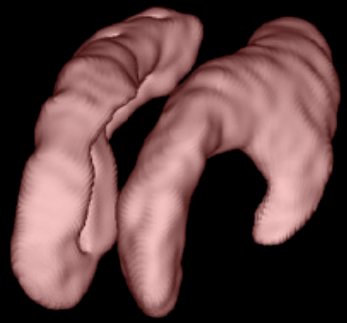

GMAT

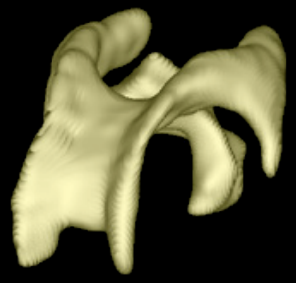

VENT

Habas et al., "Atlas-based segmentation of the germinal matrix from in utero clinical MRI of the fetal brain", Medical Image Computing and Computer Assisted Intervention, LNCS, vol. 5241, 2008.

Laminar structure of the fetal brain

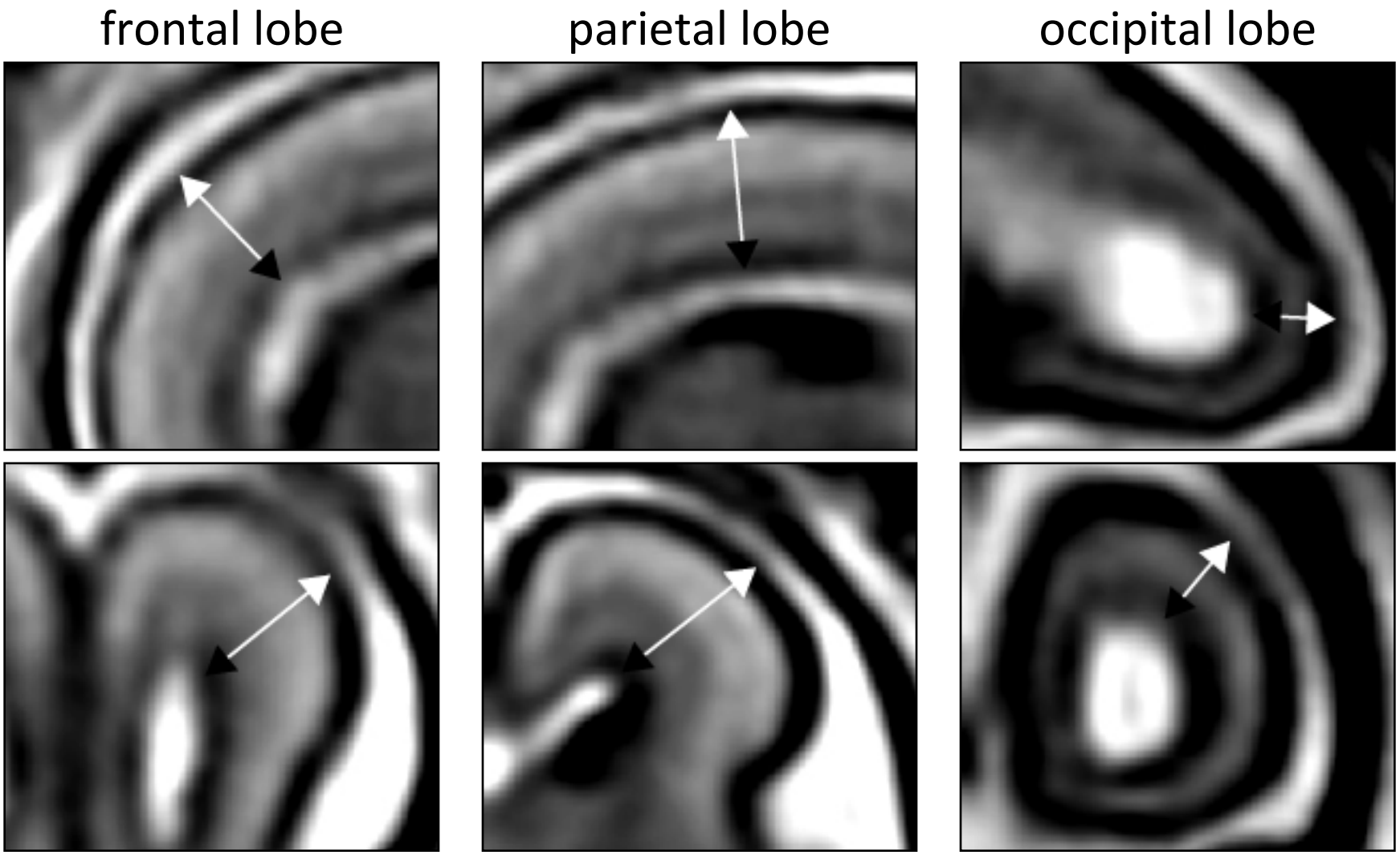

Our previous work on segmentation

- Atlas-based segmentation of the germinal

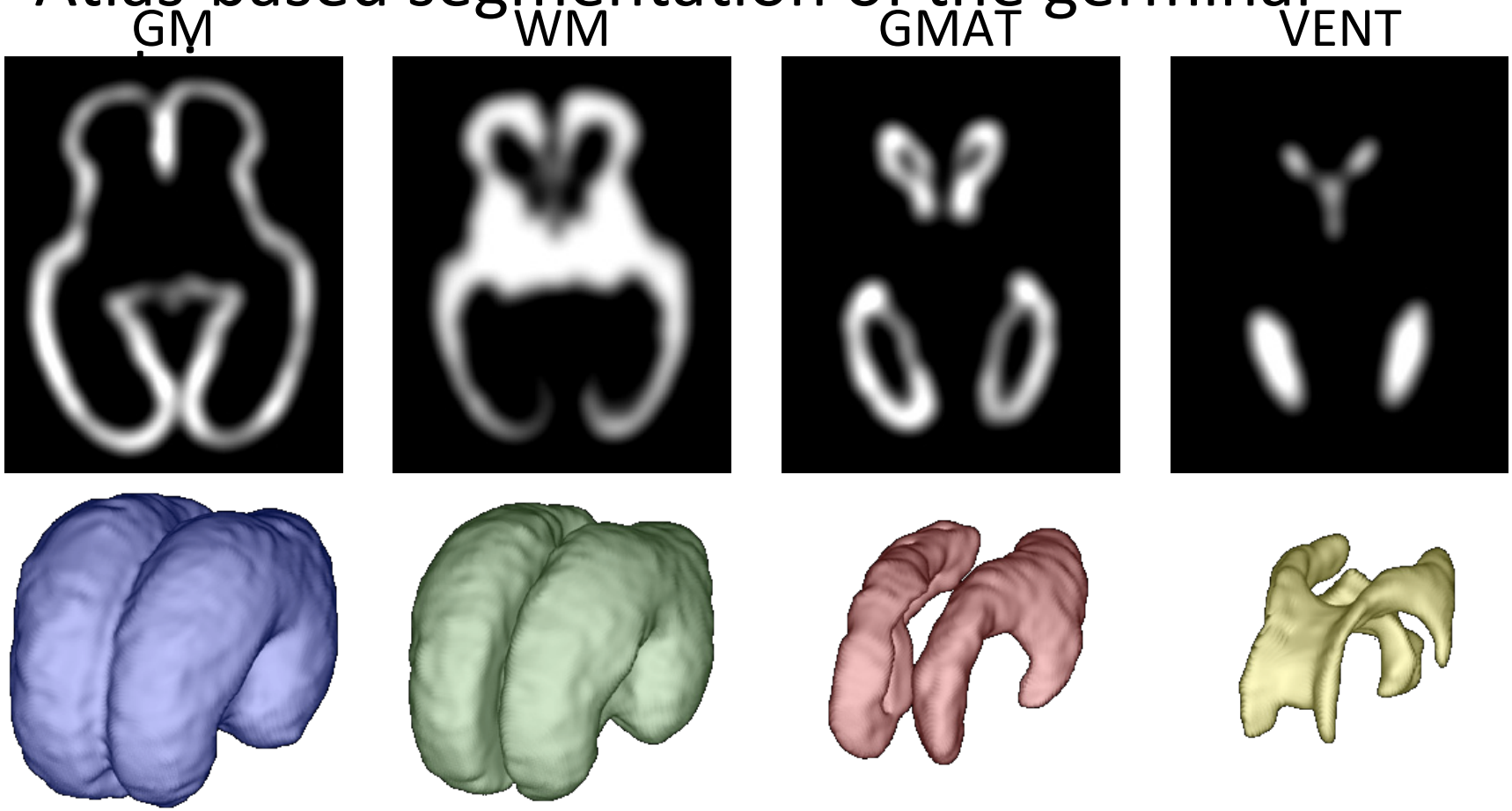

Habas et al., "Atlas-based segmentation of the germinal matrix from in utero clinical MRI of the fetal brain", Medical Image Computing and Computer Assisted Intervention, LNCS, vol. 5241, pp. 351-358, September 2008.

Depth-encoded tissue occurrence

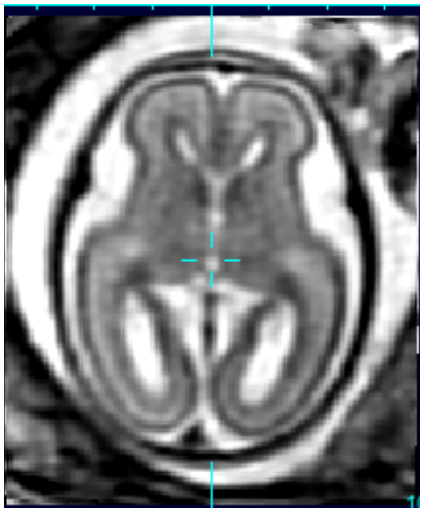

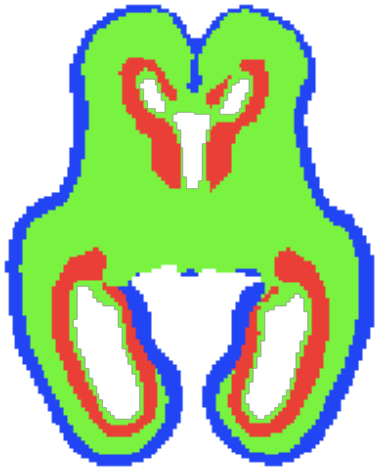

- CSF-tissue boundaries easy to find
- Tissue-tissue boundaries more fuzzy
- Different tissues occur at different depths from outer brain surface

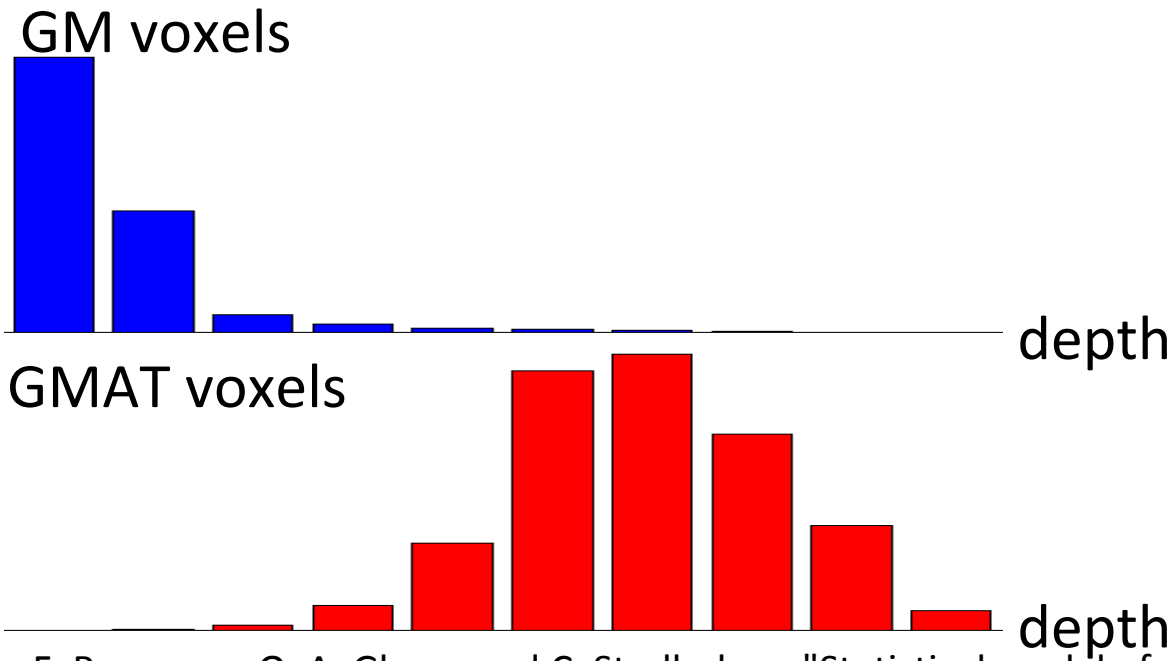

P. A. Habas, K. Kim, D. Chandramohan, F. Rousseau, O. A. Glenn, and C. Studholme, "Statistical model of laminar structure for atlas-based segmentation of the fetal brain from in-utero MR images," in Medical Imaging 2009: Image Processing, Proc. SPIE, vol. 7259, 725917, February 2009.

Laminar depth model

- Motivated by underlying process of brain growth
- Brain modeled as volume between boundary surfaces

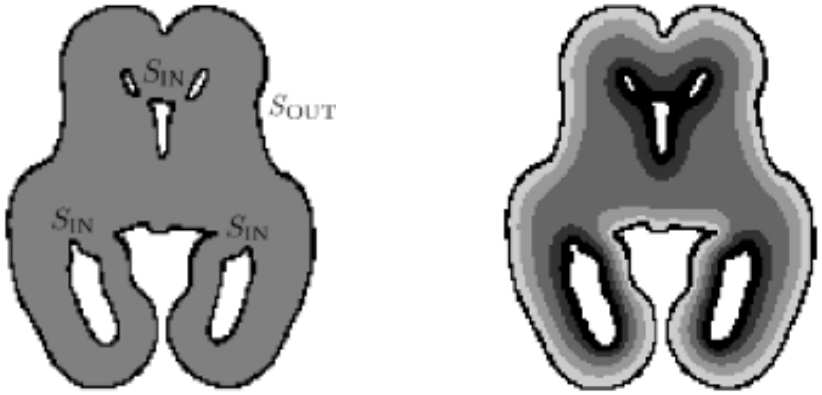

- Laminar structures can be deformed between boundaries
- Brain geometry encoded in terms of "laminar depth" from S_{OUT} towards S_{IN}

- Laminar tissue layers = nested non-intersecting layers
- Can be deformed between boundary surfaces

P. A. Habas, K. Kim, D. Chandramohan, F. Rousseau, O. A. Glenn, and C. Studholme, "Statistical model of laminar structure for atlas-based segmentation of the fetal brain from in-utero MR images," in Medical Imaging 2009: Image Processing, Proc. SPIE, vol. 7259, 725917, February 2009.

Laminar depth calculation

- Electrostatic potential distribution model
- Applied for cortical thickness mapping (Jones, 2000)
- Entire brain volume treated as potential field $\Psi(x)$
- Boundary conditions: $\Psi(S_{OUT}) = 0$ and $\Psi(S_{IN}) = 1$
- Potential distribution described by Laplace's equation

$$\nabla^2\Psi = \frac{\partial^2\Psi}{\partial x^2} + \frac{\partial^2\Psi}{\partial y^2} + \frac{\partial^2\Psi}{\partial z^2} = 0$$

- Potential value $\Psi(x)$ [0,1] used as laminar depth of x
- Iso-potential surfaces ($0 < \psi_i < 1$) divide brain volume into desired nested sublayers

P. A. Habas, K. Kim, D. Chandramohan, F. Rousseau, O. A. Glenn, and C. Studholme, "Statistical model of laminar structure for atlas-based segmentation of the fetal brain from in-utero MR images," in Medical Imaging 2009: Image Processing, Proc. SPIE, vol. 7259, 725917, February 2009.

Examples of potential distribution

boundary surfaces

potential distribution

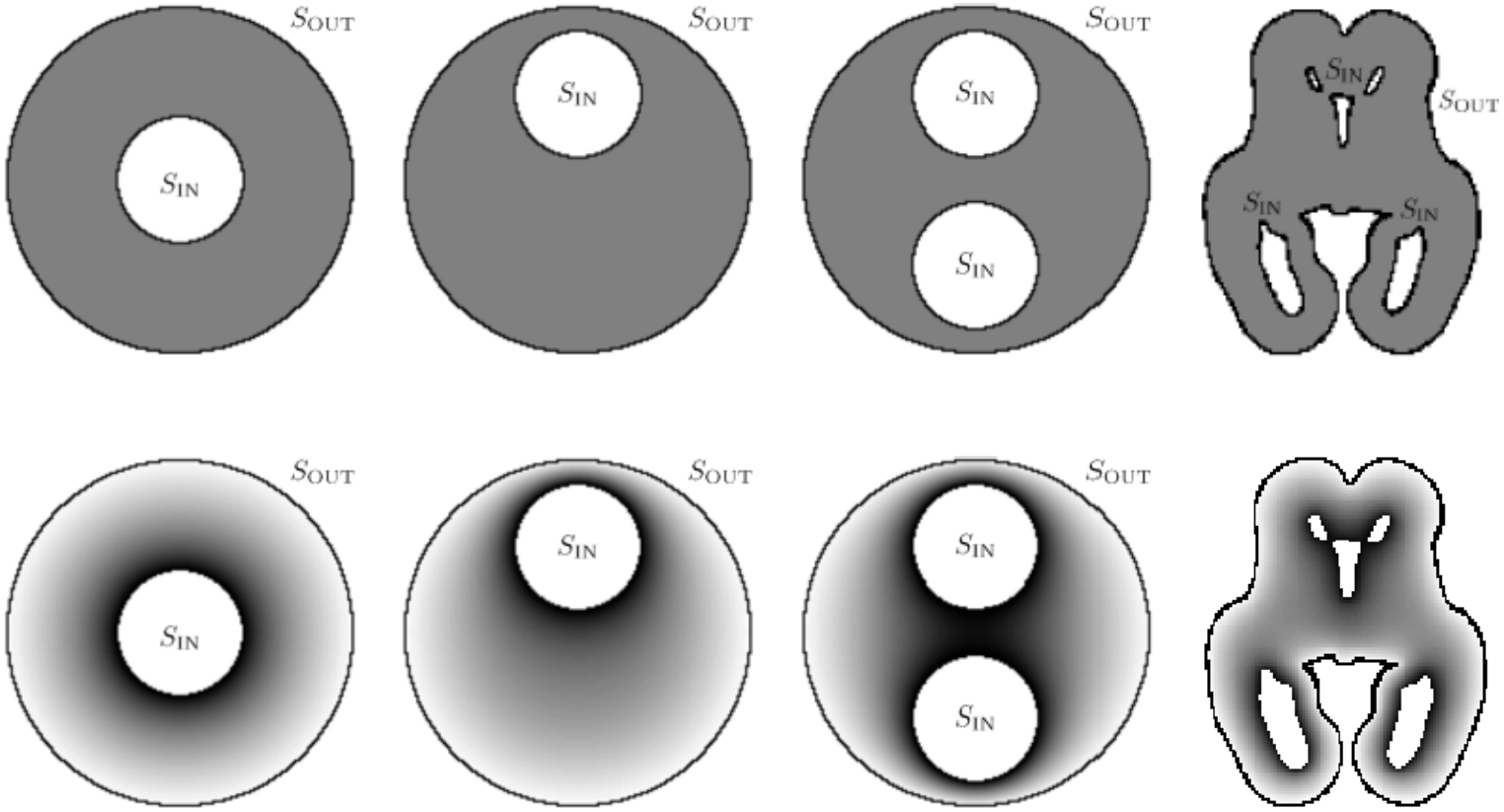

P. A. Habas, K. Kim, D. Chandramohan, F. Rousseau, O. A. Glenn, and C. Studholme, "Statistical model of laminar structure for atlas-based segmentation of the fetal brain from in-utero MR images," in Medical Imaging 2009: Image Processing, Proc. SPIE, vol. 7259, 725917, February 2009.

Laminar priors from manual segmentations

- For each level of laminar depth ψ_i and each tissue class k

$$\frac{N(\Psi(\mathbf{x}) = \psi_i, c(\mathbf{x}) = k)}{N(\Psi(\mathbf{x}) = \psi_i)} = P_L(k|\Psi(\mathbf{x}) = \psi_i)$$

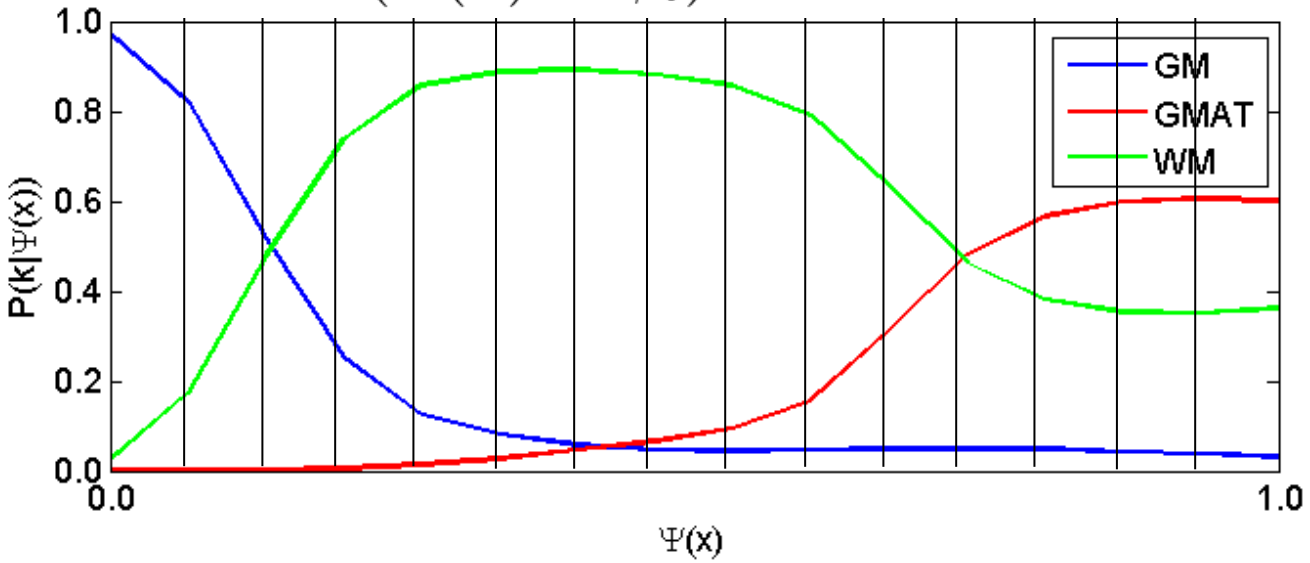

- To create complete statistical atlas of laminar structure:
  - repeat for all laminar depth levels and all tissue types
  - average over multiple subjects

P. A. Habas, K. Kim, D. Chandramohan, F. Rousseau, O. A. Glenn, and C. Studholme, "Statistical model of laminar structure for atlas-based segmentation of the fetal brain from in-utero MR images," in Medical Imaging 2009: Image Processing, Proc. SPIE, vol. 7259, 725917, February 2009.

Laminar priors for voxel classification

- To classify voxel x from a new subject:
  - use intermediate segmentation to find boundary surfaces
  - calculate $\Psi(x)$ and read priors $P_L(k|\Psi(x))$ from laminar atlas

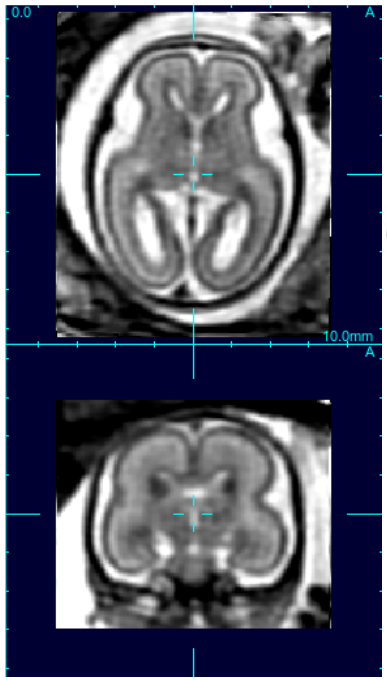

new subject

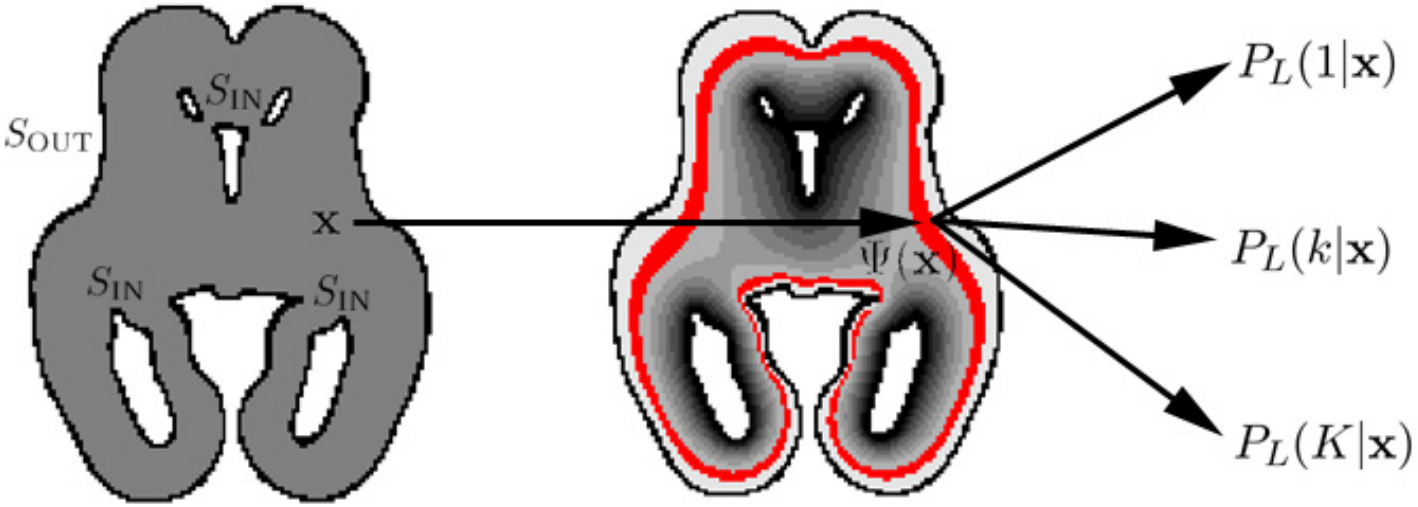

posterior probabilities $p(k|\mathbf{x}) = \frac{p(y(\mathbf{x})|k)P_L(k|\mathbf{x})}{\sum_k p(y(\mathbf{x})|k)P_L(k|\mathbf{x})}$

Laminar atlas-based EM segmentation

- Conventional statistical prior, $P_A(k|x)$
  - derived from anatomical 3D atlas
  - spatially-varying
  - spatial constraints for segmentation

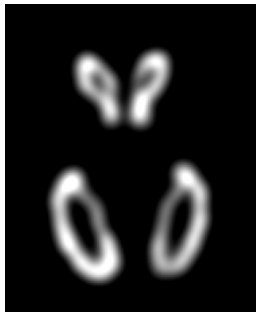

- Laminar prior, $P_L(k|\Psi(x)) = P_L(k|x)$
  - derived from laminar 1D atlas
  - depth-varying
  - additional constraints on tissue labels

- Combined prior for laminar atlas-based EM segmentation

$$P(k|\mathbf{x}) = \frac{P_A(k|\mathbf{x})P_L(k|\mathbf{x})}{\sum_k P_A(k|\mathbf{x})P_L(k|\mathbf{x})}$$

Segmentation

- Images manually segmented into GM, GMAT, WM, VENT
- Registered to common reference space (linear + elastic)
- Conventional atlas-based EM segmentation, EM(P_A)
  - K = 6 (GM, GMAT, WM, VENT, 2 x non-brain)
  - Gaussian intensity distributions, $\Theta_k = \{\mu_k, \sigma_k\}$
  - Initial values of μ_k and σ_k calculated using probabilistic atlas
  - Prior probabilities from anatomical 3D atlas, $P(k|x) = P_A(k|x)$
  - Convergence after 20-30 iterations
- Laminar atlas-based EM segmentation, EM(P_A+P_L)
  - Laminar depth recalculated from in each iteration
  - Combined priors used for class probability estimation

Segmentation results

- Whole brain, sagittal view

reconstructed motion-corrected MRI

EM segmentation with prob. atlas

after refinement with laminar priors

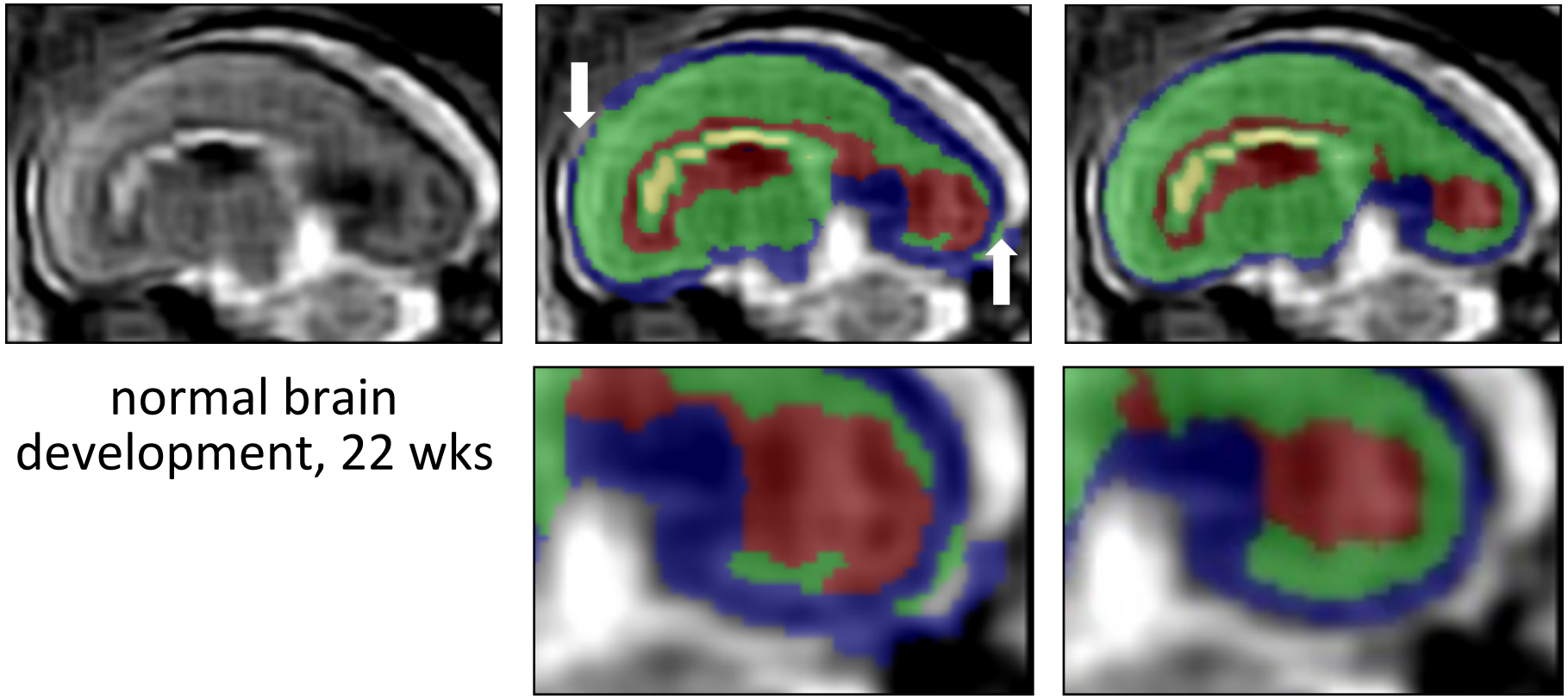

normal brain development, 22 wks

P. A. Habas, K. Kim, D. Chandramohan, F. Rousseau, O. A. Glenn, and C. Studholme, "Statistical model of laminar structure for atlas-based segmentation of the fetal brain from in-utero MR images," in Medical Imaging 2009: Image Processing, Proc. SPIE, vol. 7259, 725917, February 2009.

Segmentation results

- Occipital lobe, coronal view

reconstructed motion-corrected MRI

EM segmentation with prob. atlas

after refinement with laminar priors

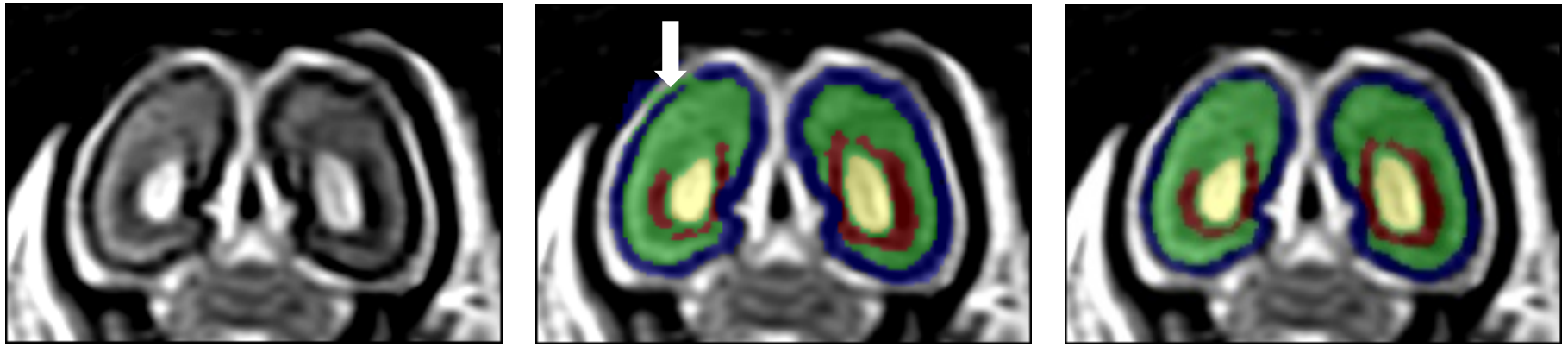

normal brain development, 22 wks

P. A. Habas, K. Kim, D. Chandramohan, F. Rousseau, O. A. Glenn, and C. Studholme, "Statistical model of laminar structure for atlas-based segmentation of the fetal brain from in-utero MR images," in Medical Imaging 2009: Image Processing, Proc. SPIE, vol. 7259, 725917, February 2009.

Quantitative validation

- Automatic segmentations evaluated in terms of DSC with respect to reference manual segmentations
  - manual vs. conventional atlas-based segmentation EM(P_A)
  - manual vs. laminar atlas-based EM segmentation EM(P_A+P_L)
- DSC values averaged over all study subjects

tissue	whole brain		par. & occ. lobes	
	EM(P_A)	EM(P_A+P_L)	EM(P_A)	EM(P_A+P_L)
GM	0.77 ± 0.03	0.76 ± 0.03	0.81 ± 0.02	0.82 ± 0.02
GMAT	0.73 ± 0.03	0.73 ± 0.03	0.71 ± 0.02	0.73 ± 0.02
WM	0.85 ± 0.03	0.87 ± 0.03	0.81 ± 0.01	0.87 ± 0.01

Summary

- Described the basic approach to Automated Brain Tissue labeling using in many MRI studies
- Examined two extensions to the approach that specifically deal with challenges of the developing brain:
  - The use of Subject(Age) specific priors that can be parameterized to better match a new subject MRI
  - The use of an anatomy specific geometry in which to define priors

P. A. Habas, K. Kim, D. Chandramohan, F. Rousseau, O. A. Glenn, and C. Studholme, "Statistical model of laminar structure for atlas-based segmentation of the fetal brain from in-utero MR images," in Medical Imaging 2009: Image Processing, Proc. SPIE, vol. 7259, 725917, February 2009.

Quantifying Early Human Brain Tissue Growth:

How to build a complex brain from a simple brain?

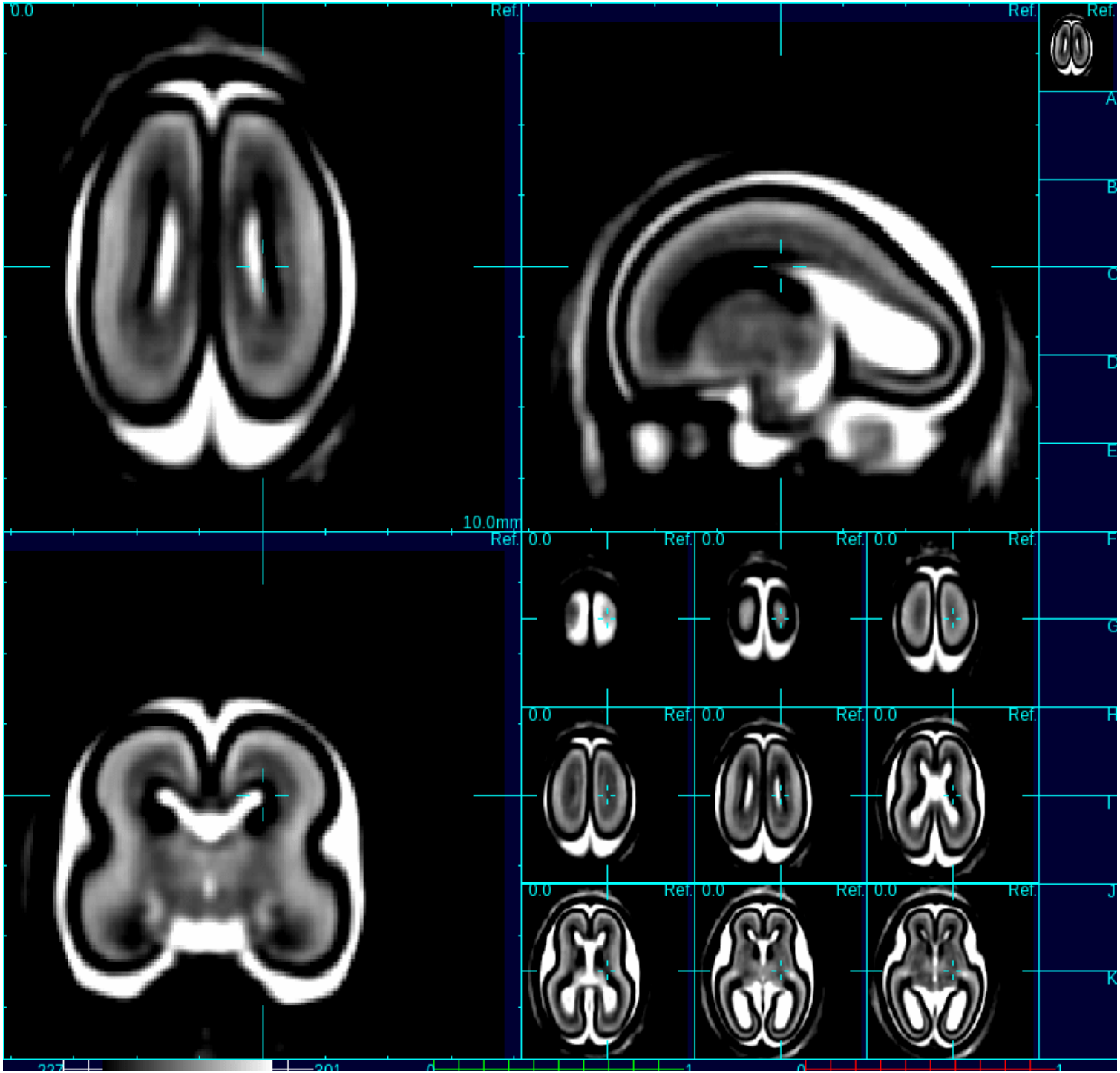
0.0
Ref.
10.0mm
A
B
C
D
E
F
G
H
I
J
K

Early Human Brain Growth 21-28W

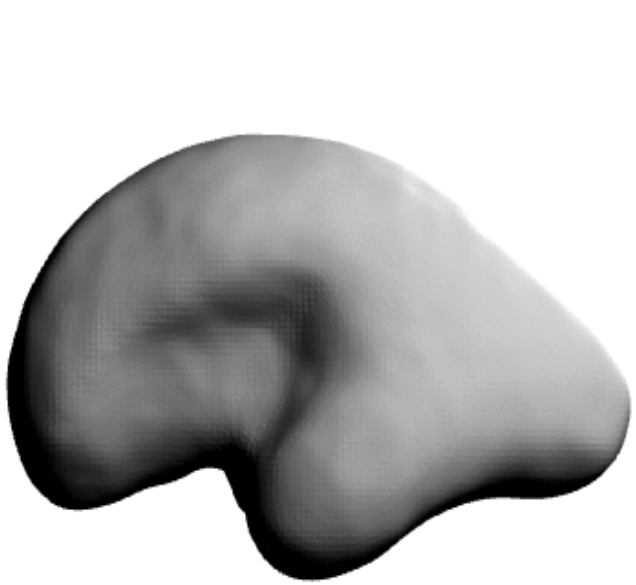

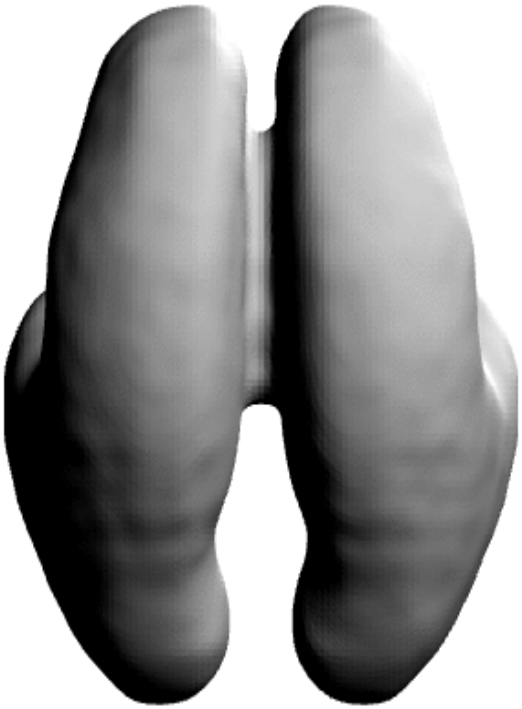

21 22 23 24 25 26 27 28

Measuring Human Fetal Brain Growth

Motivation: Study of Early Brain Growth:

- Smooth Brain -> Primary sulci+gyri
- Structural Complexity requires Local differential growth patterns

->Need to add tissue at different rates at different anatomical locations

Here we map these patterns using TBM to look at internal growth patterns

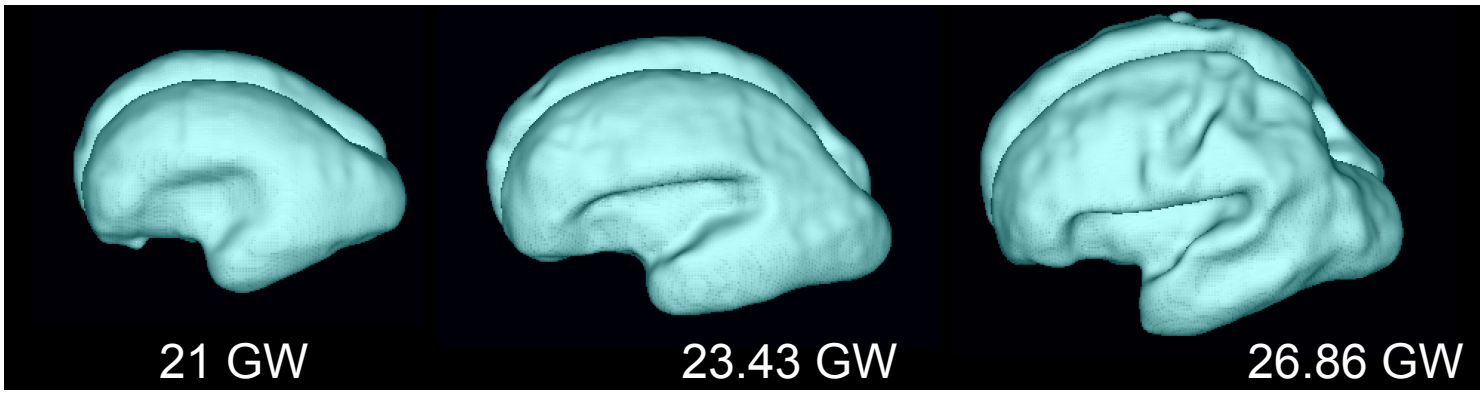

Statistical Modeling of Local Anatomical Size Across A Population with different ages:

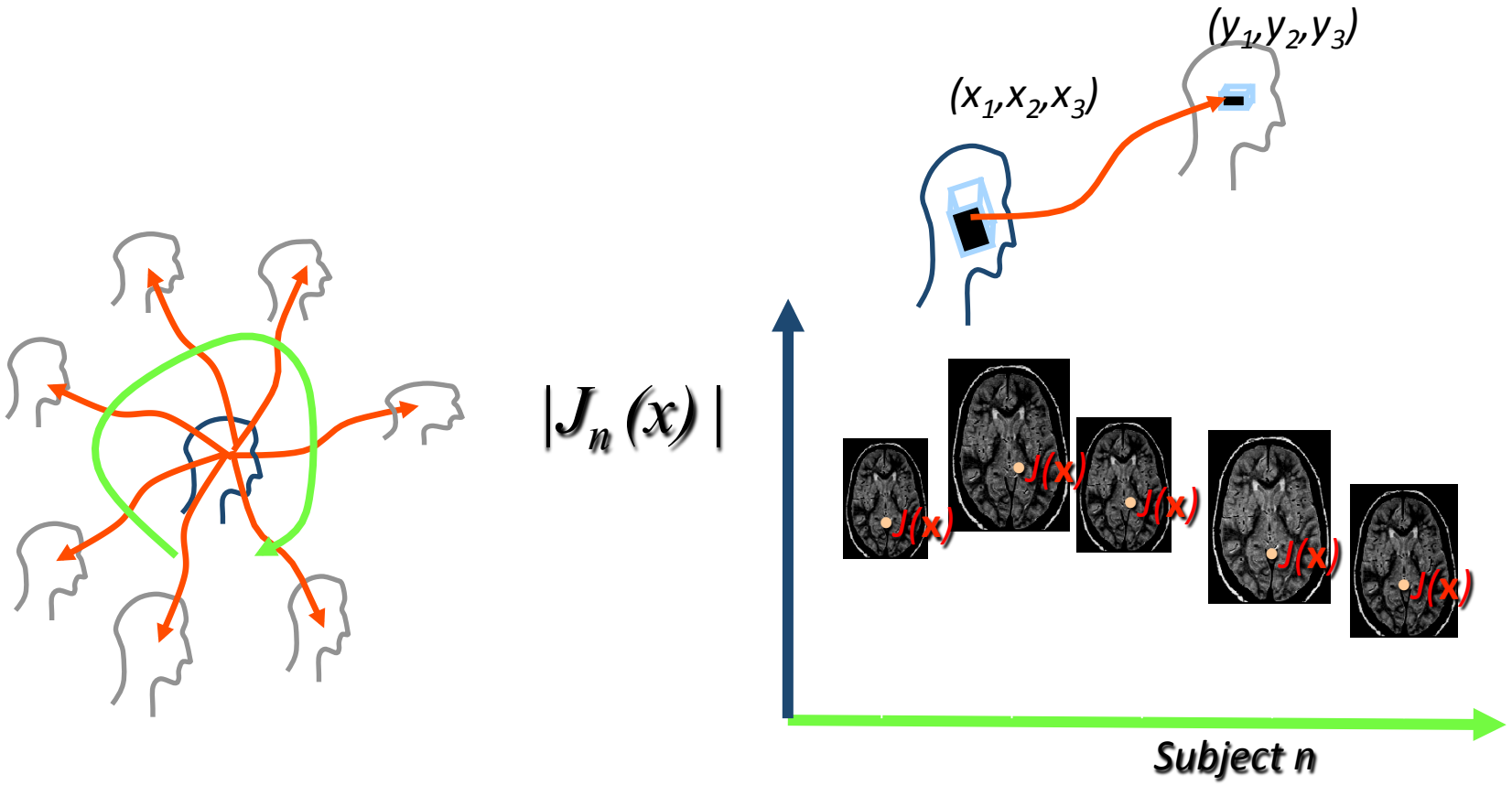

Linear regression to test for voxels with significantly greater or lesser expansion than that of the whole brain

Growth Rate Map

Weekly growth rate relative to global rate of STV increase

V. Rajagopalan et al, "Local tissue growth patterns underlying normal fetal human brain gyrification quantified in utero," J. Neurosci., vol. 31, no. 8,

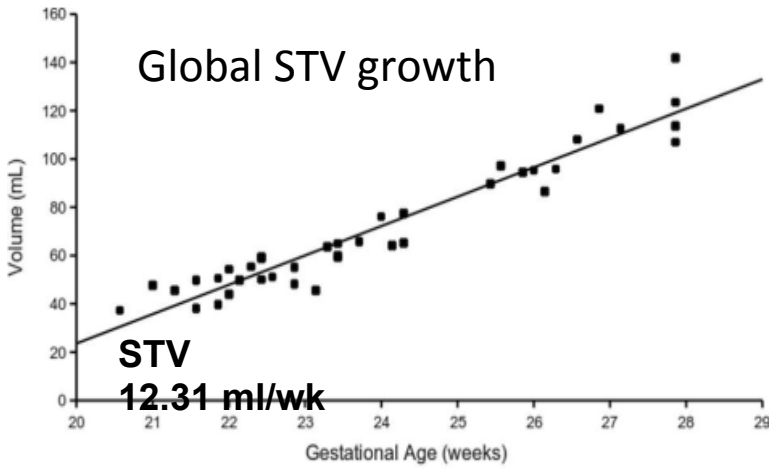

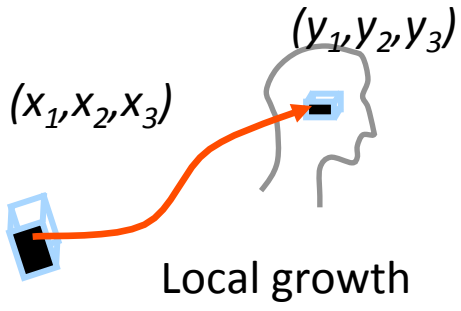

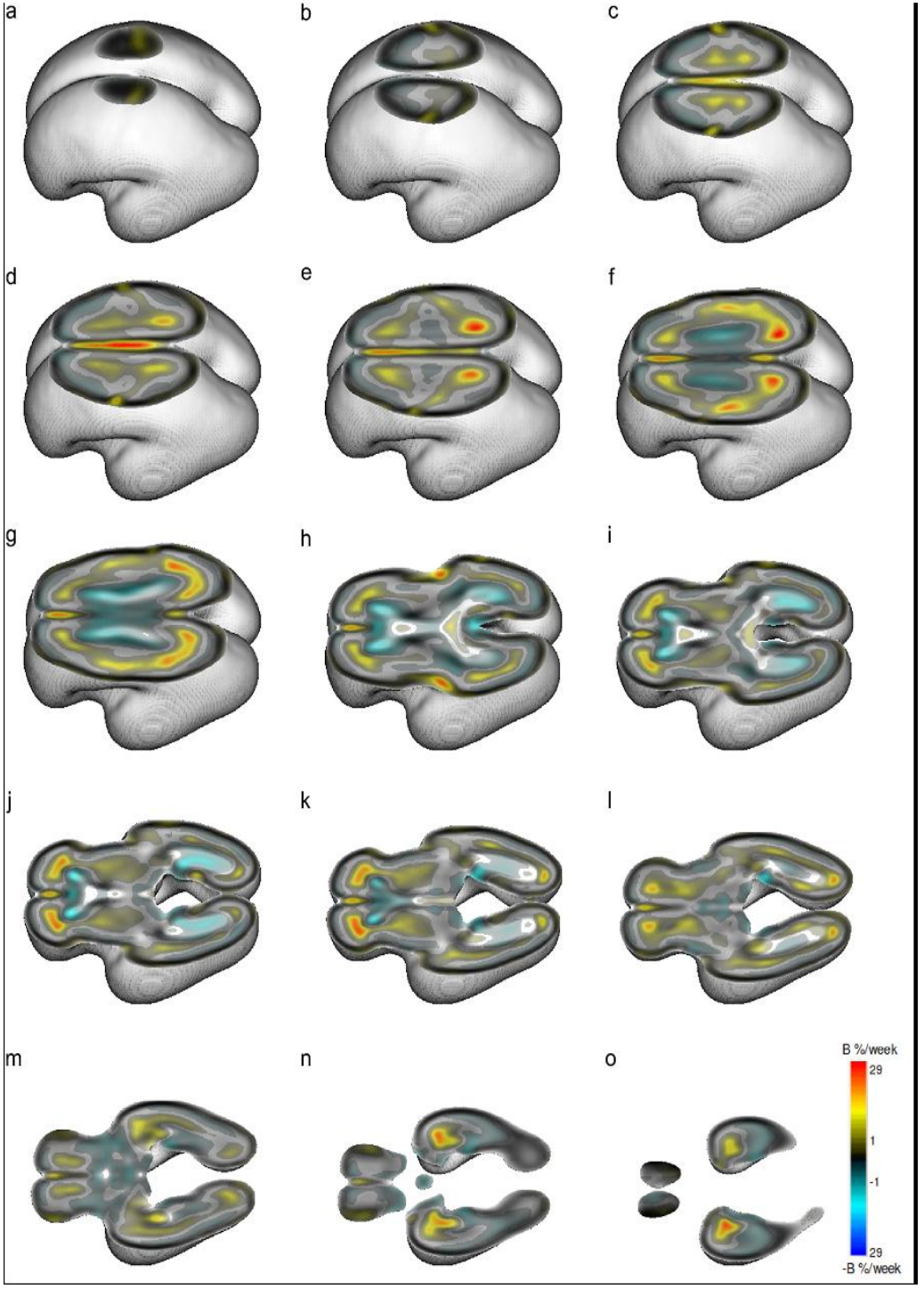

ROI growth trajectories

Sulcal/gyral gray matter growth is accelerating

White matter growth is linear

Bilaterally symmetrical growth rates

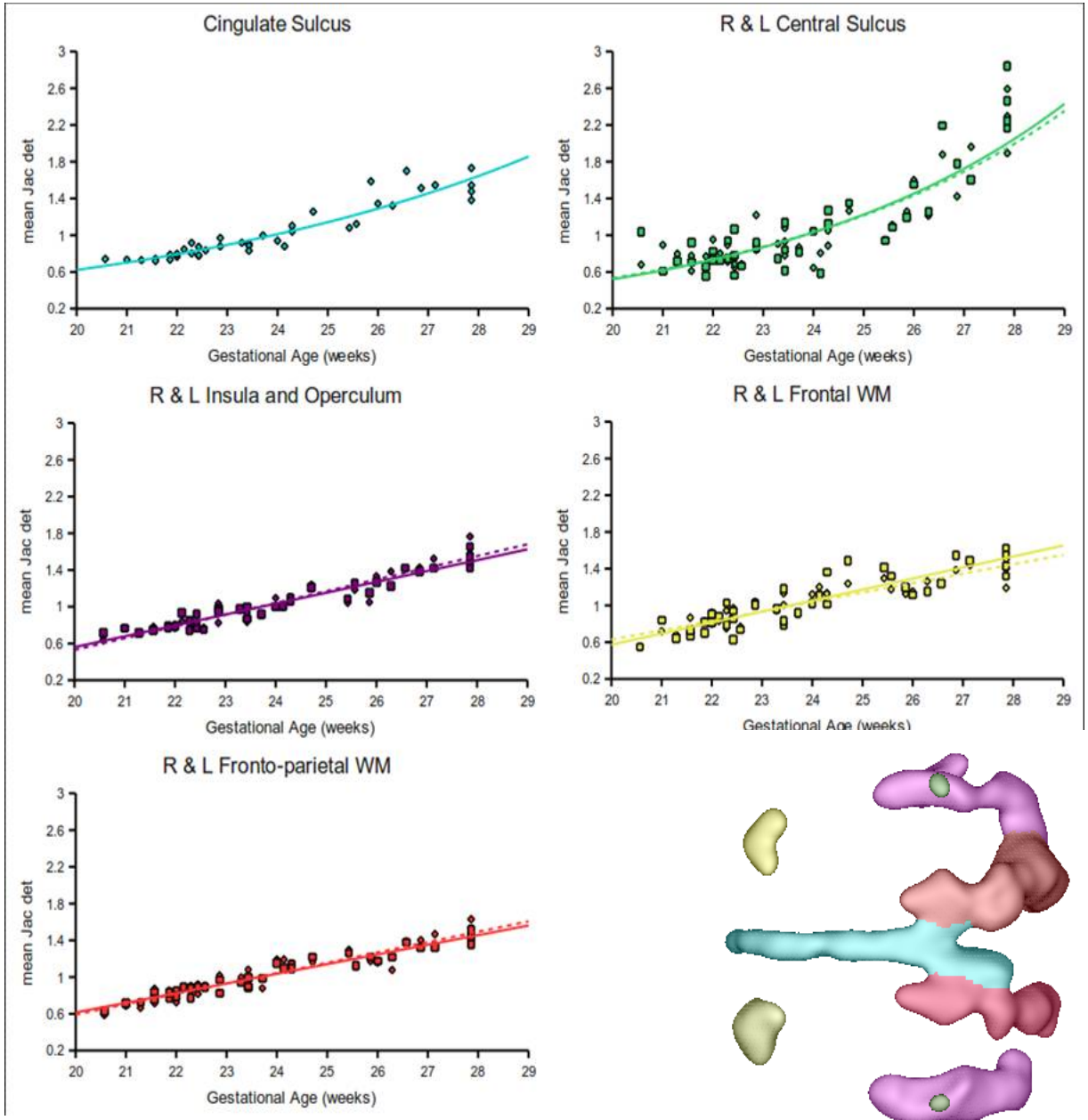

V. Rajagopalan et al, "Local tissue growth patterns underlying normal fetal human brain gyrification quantified in utero," J. Neurosci., vol. 31, no. 8,

CP: Local Area + Thickness increases

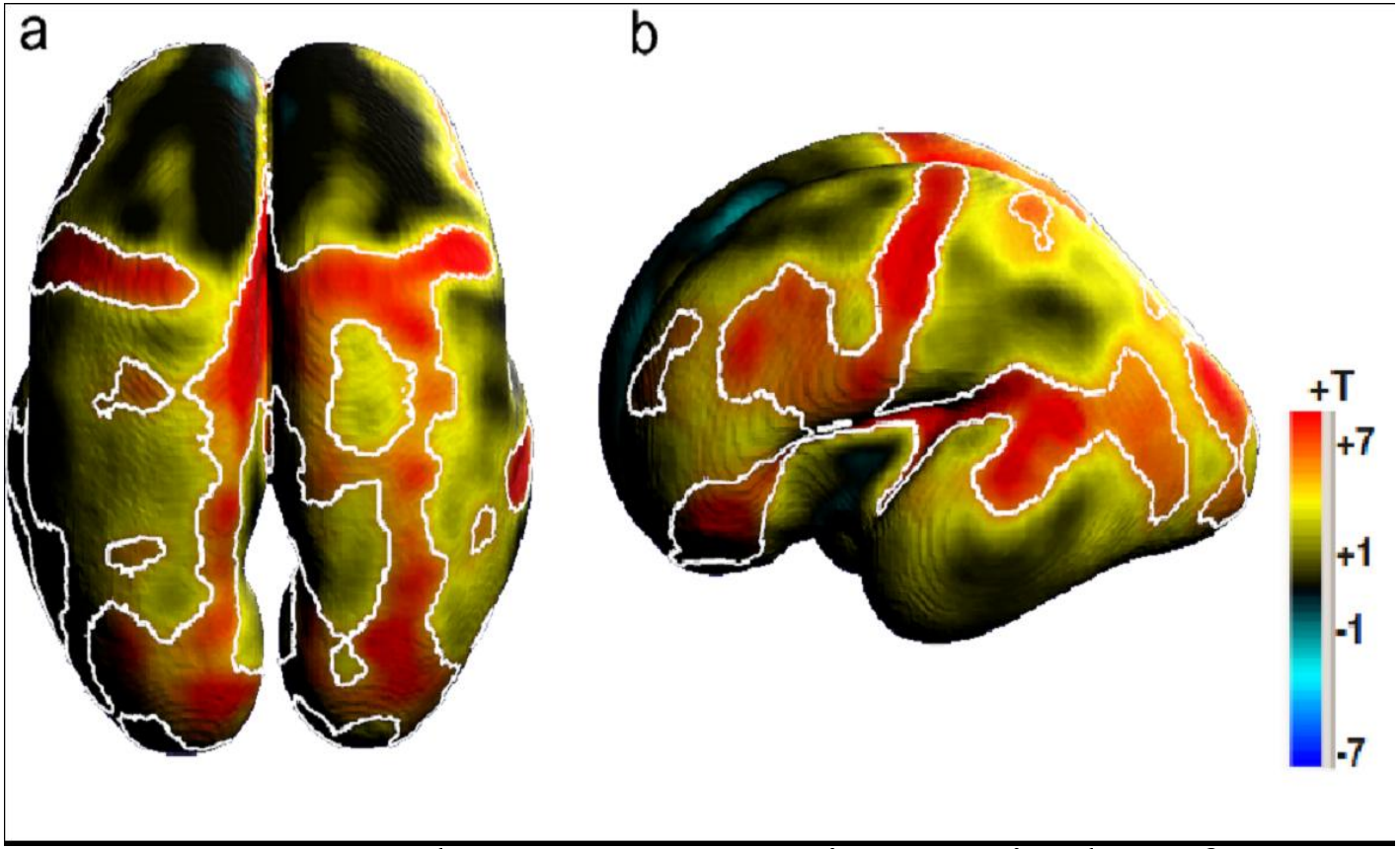

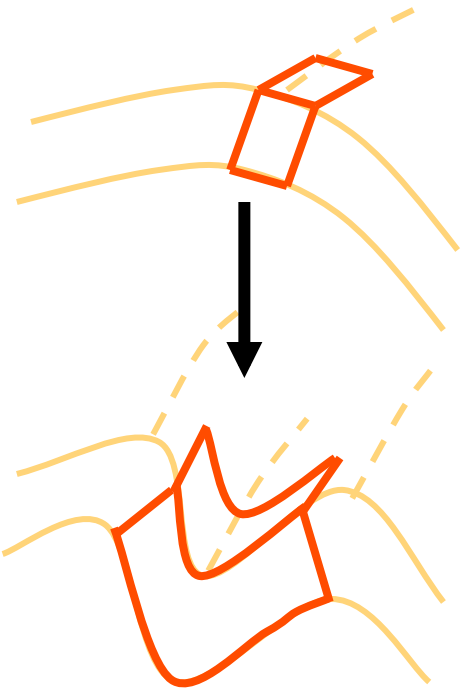

Greater growth rate on posterior cortical surface
Central, superior temporal and circular sulci emergence

V. Rajagopalan et al, "Local tissue growth patterns underlying normal fetal human brain gyrification quantified in utero," J. Neurosci., vol. 31, no. 8,

Mapping and Quantifying Human Fetal Brain Folding

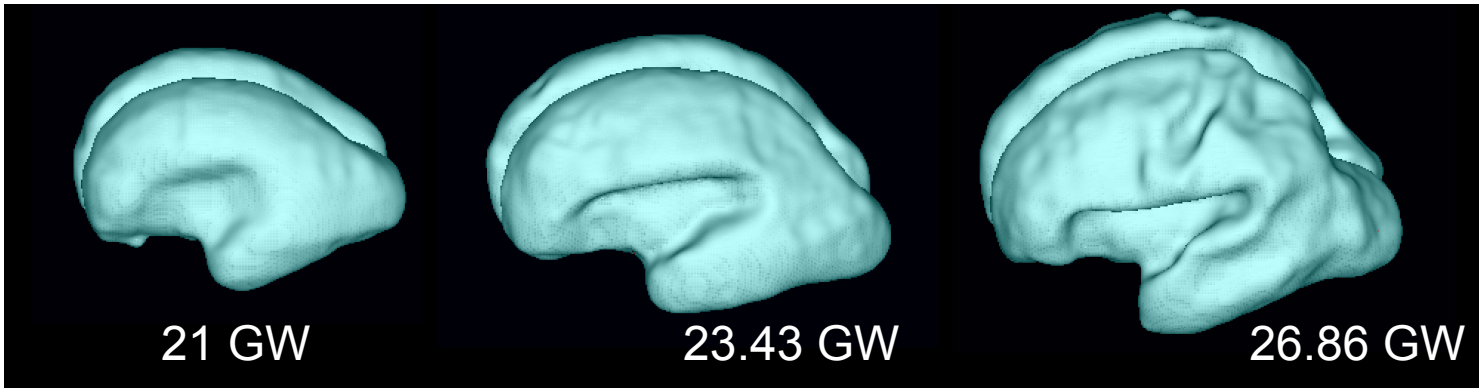

- Maximal and minimal curvature k1, k2
  - Mean curvature: H=(k1+k2)/2
  - Gaussian curvature: K=k1*k2
  - Curvedness (Koenderink 1992)
  - Shape index (Koenderink 1992)
  - Bending energy (van Vliet 1993)

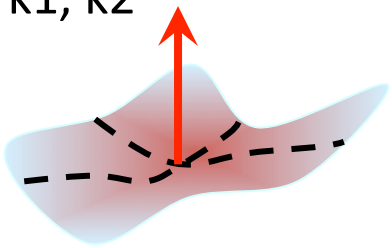

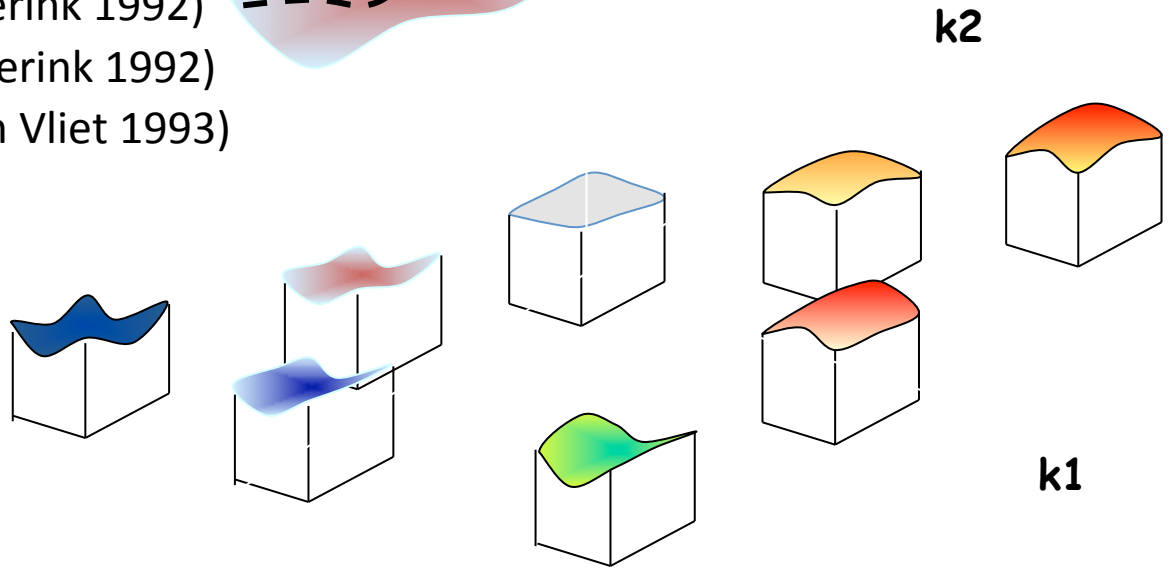

Detecting Statistically Significant Changes of Curvature

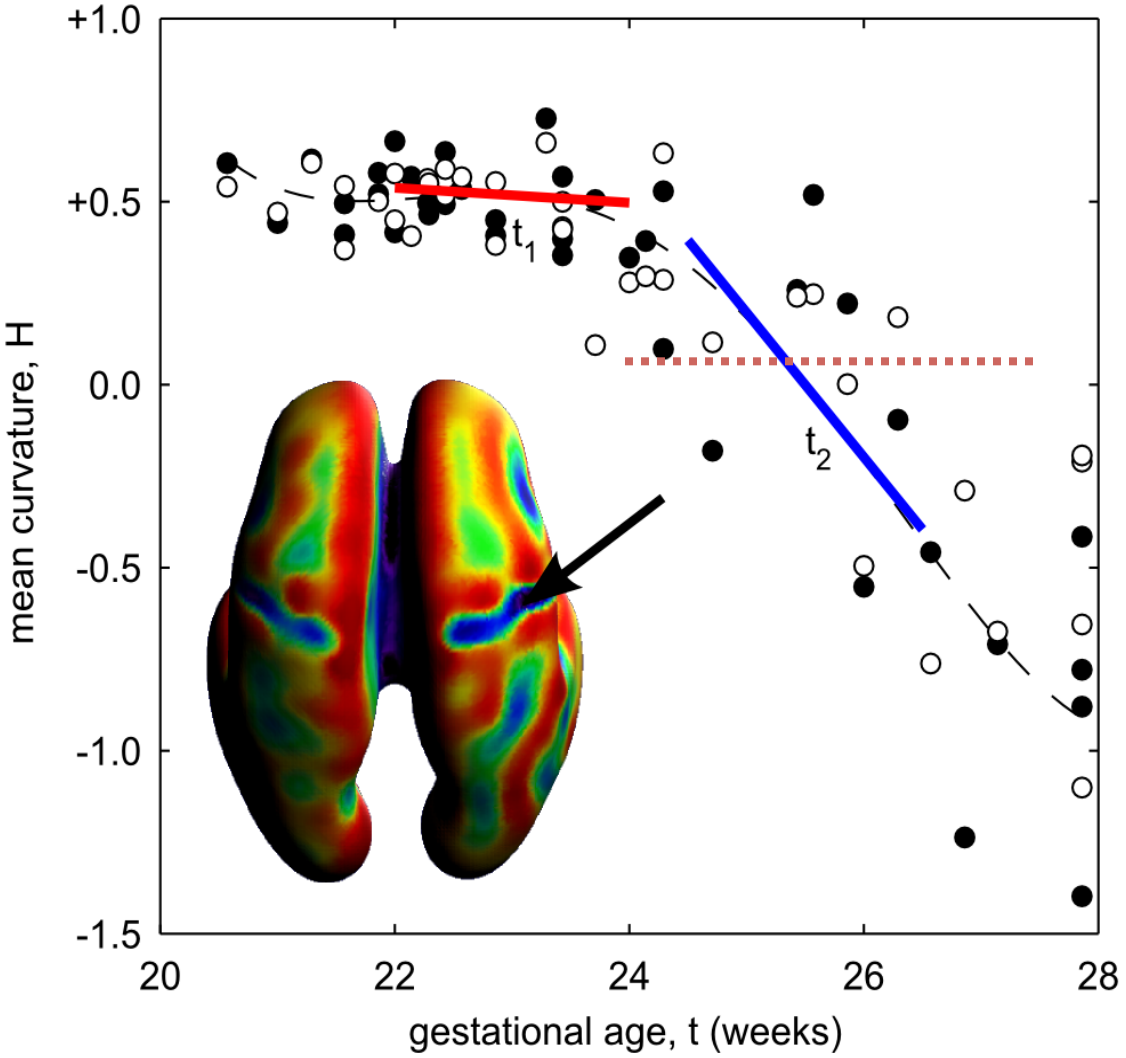

P. A. Habas, et al, "Early folding patterns and asymmetries of the normal human brain detected from in utero MRI," Cereb. Cortex, online, in press.

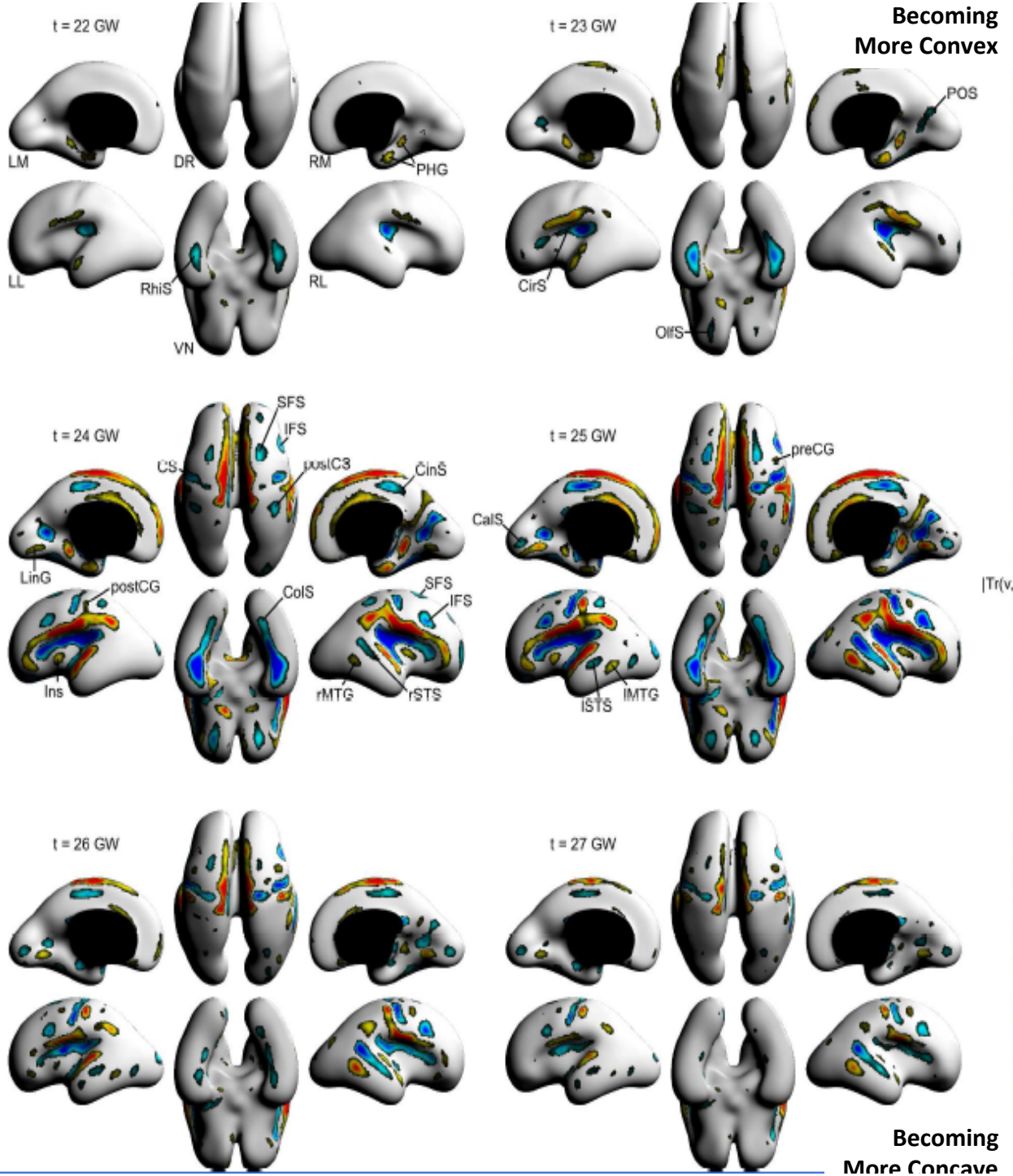

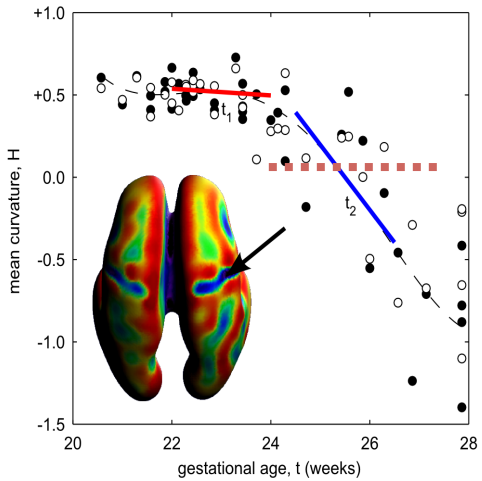

T Maps of **where** and **when** (statistically)

$$\frac{dH(v)}{d(t)} > 0$$

or

$$\frac{dH(v)}{d(t)} < 0$$

P. A. Habas, et a Cereb. Cortex, online, in press.

All maps are thresholded at significance level

The Emergence of Asymmetry in Surface Curvature

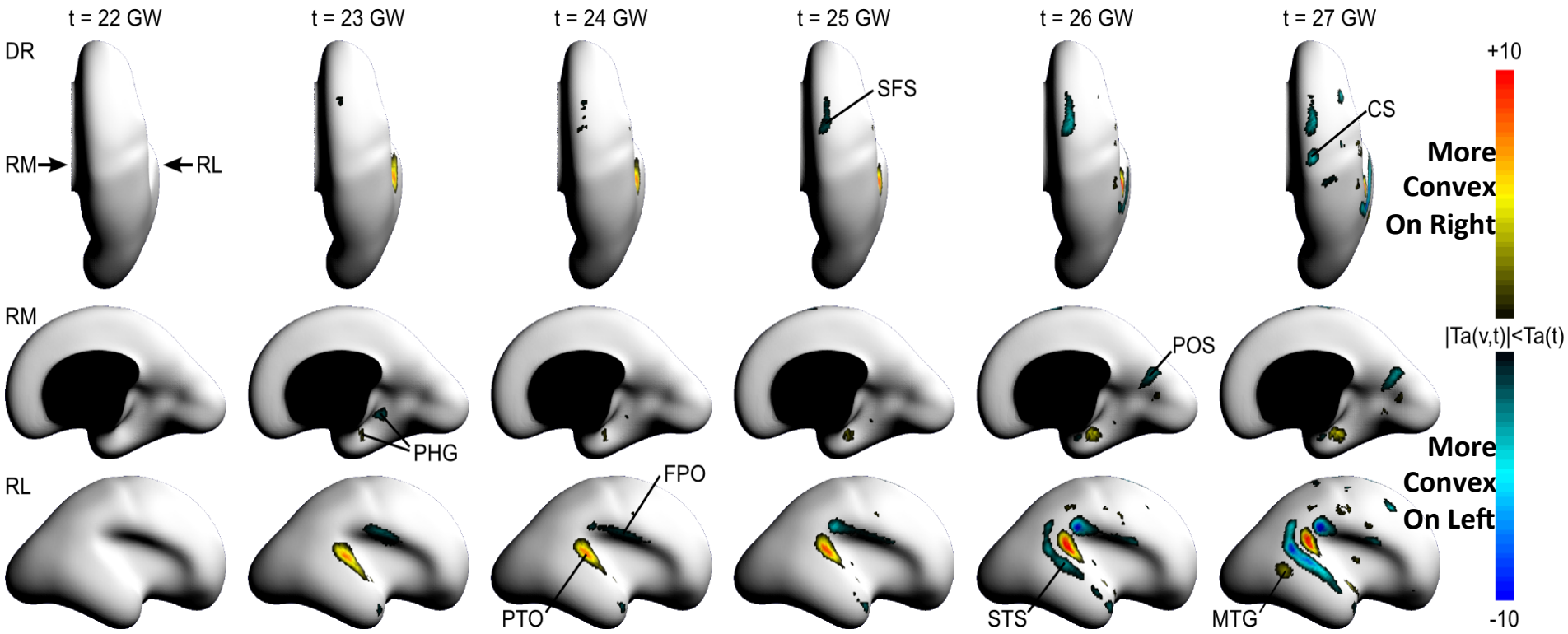

Maps of the fetal brain surface where there are significant inter-hemispheric curvature asymmetries at a given voxel

All maps are thresholded at significance level p = 0.05 (corrected).

P. A. Habas, et al Cereb. Cortex, online, in press.

Folding delays in IMVMs

- Significant sulcation delays detected bilateraly in regions of the parieto-occipital sulcus

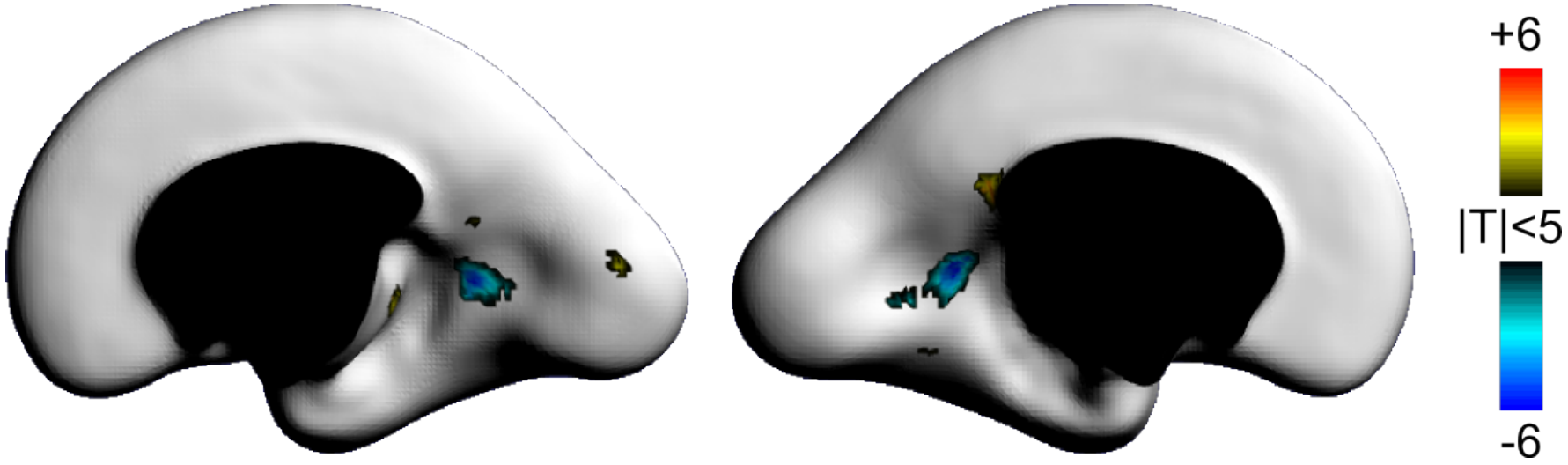

Acknowledgements

Funding: NIH Grant R01 NS 055064 (PI: Colin Studholme)

Current Postdocs:

- Kio Kim, Piotr Habas,
- Vidya Rajagalopalan, Julia Scott
- Mads Fogtmann Hansen,
- Sharmishtaa Seshamani
- Current Rotation/Visiting PhD Students:
  - Erzhuo Wang
- Undergraduate Summer Students:
  - Averi Kitsch, Anupama Ramakrishnan
  - Dharshan Chandramohan, Ahmad Roosta,
  - Nathan Volman
- Collaborators:
  - UCSF: Orit Glenn, Jim Barkovich
  - Strasbourg: Francois Rousseau, Meriam Koob, Jean-Louis Dietemann,
  - Vancouver: Steven P. Miller, Ashley J. Robinson, Kenneth J. Poskitt

Review of fetal imaging work:

Mapping fetal brain development in utero using MRI: the big bang of brain mapping

Annu. Rev. Biomed. Eng., vol. 13, no. 1, pp. 345-368, August 2011.

Lots of Projects for interested students!

Visit website: http://depts.washington.edu/bicg

email me: colin.studholme@ieee.org